5-2018

Fibers for Skin Regeneration

Astrid Michelle Rodriguez Negron
The University of Texas Rio Grande Valley

FIBERS FOR SKIN REGENERATION

A Thesis

by

ASTRID MICHELLE RODRIGUEZ NEGRON

Submitted to the Graduate College of
The University of Texas Rio Grande Valley
In partial fulfillment of the requirements for the degree of

MASTER OF SCIENCE ENGINEERING

May 2018

Major Subject: Mechanical Engineering

FIBERS FOR SKIN REGENERATION

A Thesis
by
ASTRID MICHELLE RODRIGUEZ NEGRON

COMMITTEE MEMBERS

Dr. Karen Lozano
Chair of Committee

Dr. Robert Gilkerson
Co-Chair of Committee

Dr. Rogelio Benitez
Committee Member

May 2018

ABSTRACT

Rodriguez Negron, Astrid Michelle, Fibers for Skin Regeneration. Master of Science Engineering (MSE), May 2018, 81 pp, 4 tables, 28 figures, 117 references, 38 titles.

This thesis presents the successful development of biocompatible Polyvinyl Butyral (PVB), PVB/Polylysine and PVB/Tannic Acid (TA)/Polylysine fibers from an ethanol solution, Polyhydroxybutyrate (PHB), PHB/Polylysine, PHB/TA/Polylysine fibers from a chloroform solution and Chitosan (CH)/Pullulan (PL)/TA and CH/PL/TA/Polylysine fibers from an aqueous solution. The fibers were mass produced utilizing the Forcespinning® (FS) technology. The morphology of the fibers was characterized using a scanning electron microscope (SEM) and the fibers average diameter was calculated. The thermal properties of the fibers were characterized using a thermogravimetric analyzer (TGA) and a differential scanning calorimeter (DSC). The antibacterial activity of the fibers was assessed using against *Escherichia coli*. The biocompatibility of the fibers was studied by culturing NIH 3T3 Mouse Embryonic Fibroblast cells in the fibers. These fibers provide the cells with a 3D environment mimicking the extracellular matrix (ECM) in the skin which favors cell adherence and attachment, thus favoring skin wound healing.

DEDICATION

I would like to dedicate this work to the people that one way or another made this possible. To my mentors, my family and friends for all the support. My dad, Victor Rodriguez Rosario, and my mom, Rosa Maria Negron Candelaria, from a distance and my little brother, Victor Andres Rodriguez Negron, that I have missed dearly during my stay so far away from home. Papi, mami y Andres: gracias por todo, los amo.

ACKNOWLEDGMENTS

I will always be grateful to Dr. Karen Lozano, chair of my thesis committee, for her mentorship, help and ideas, which without them this thesis wouldn't exist. Dr. Lozano gave me the opportunity to learn about polymers in a somewhat extensive way and she gave me the confidence that I needed to cross this finish line. May you live long and inspire as many as you inspired me. I will always be thankful to Dr. Robert Gilkerson, co-chair of my thesis, for all his mentoring and advice. Also thank you for all the help with the cell growth experiments. My thanks go as well to Dr. Rogelio Benitez, for his input and advice which helped ensure the quality of my work. To my committee: thanks for the opportunity to learn, the funding and all their time spent helping me understand my research, results, and revising and editing my manuscript. Thank you for the patience, encouragement and guidance.

Special thanks for the help and work of Luissanyi Campos and Cristobal Rodriguez for their help in characterization of the material and cell growth experiments, respectively. I am also grateful to Dr. Luis A. Materon for helping me with the bacterial experiments.

I would like to acknowledge Partnership for Research in Materials NSF Grant, Mrs. Lisa Moreno, Dr. Akia, Mrs. Victoria Padilla and Dr. Karen Baylon for their extended help during my years as a master's student

TABLE OF CONTENTS

Page

LIST OF TABLES

Page

LIST OF FIGURES

Page

CHAPTER I

INTRODUCTION

This thesis discusses the development and characterization of fine fiber membranes made by the Forcespinning® (FS) technology to improve skin cell growth and facilitate skin regeneration for burn victims, diabetic wounds, and other acute skin injuries. Current technology to treat these lesions varies from patient to patient and from one skin injury to another.

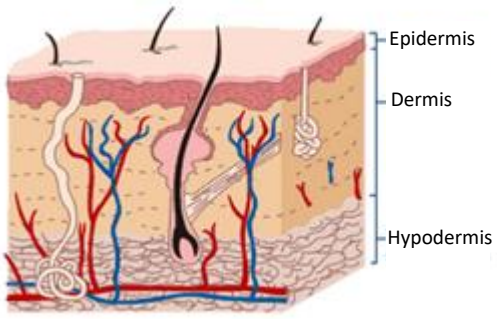

Figure 1. Diagram of the skin [1]

The skin is the largest organ in the human body, its job or function is to protect the other organs from the environment acting as a barrier that keeps the body temperature and fluids inside the body and keeps exogenous organisms out of the body. The skin is divided into three main layers the epidermis, the dermis and hypodermis (Figure 1.).

Acute skin injuries, referring to wounds located in the dermis or hypodermis where the capillaries and nerves are located, are susceptible to infections, loss of heat, and loss of fluids.

Most of the treatments for these types of injuries include long hospitalization times and constant health care giver supervision that oversee general day to day treatment, change and bandage of the exposed skin injury, and administration of pain medication and antibiotics. There are many complications that may arise from lack of, or improper treatment, or from human error as in the injury needs to be treated and cared by a health specialist whose responsibility is to maintain it clean and in optimum conditions for cell growth and healing. As mentioned most of the complications are infections with viruses, bacteria or any pathogens present in the environment that can grow in the exposed area, loss of body heat, and inappropriate scarring, among others. There are many studies on skin regeneration and wound healing. The utilization of polymers that are biocompatible and have the ability to form fiber scaffolds is widely studied for applications that involves cell growth and regeneration in bones, muscles, and other organs. This thesis studies the fabrication of fiber membranes through the Forcespinning® technology for cutaneous wound healing. The polymer fibers are known to mimic the extracellular matrix which allows cell growth in a 3D format speeding up the healing of the wound. Even though there are studies that show the advance in wound healing using fibers, the most studied technique to get those fibers have a low yield thus making it difficult and extremely expensive to mass produce the fiber membranes. However, the Forcespinning® technology have a higher yield and possibilities of mass producing fibers without the excessive costs to further promote the use of fibers in the medical field.

The need of a rapid healing process or a device that could improve healing after an acute skin injury is required for better healing and it is desired to decrease healing time and pain. This thesis focuses on the development and characterization of the fiber membranes and its corresponding three-dimensional cell growth/proliferation and antimicrobial studies.

This thesis is divided into six chapters. Chapter two focuses on the literature review, it discusses the current technology and the research being done in the field of skin wound healing and skin regeneration. It discusses the biology behind wound healing, the skin parts and the different technologies being studied such as the use of hydrogels, scaffolds, different antimicrobial agents, and nanotechnology to improve wound healing and reduce the risk of infection and other complications.

Chapter three describes the equipment used within the experimental work. The techniques and instrumentation required to fulfill the development of the material, its characterization, and cell growth and antimicrobial experiments. Among the described instruments/techniques are the Forcespinning® technology, the scanning electron microscope, thermal characterization instruments, incubator, and fluorescence microscopes.

Chapter four discusses the materials and methods used. The specification of each material, its supplier and modifications, how the solutions were prepared, how the fibers were obtained, and the settings used to spin the solutions into fibers. The characterization of the material: thermal, morphological, and biological, as well as experiments performed to obtain data are well described.

Chapter five presents the results and discussion followed by Chapter six which highlights the conclusions obtained from the development and characterization of the membranes. Suggestions for future work are also presented in Chapter six.

The thesis entitled “Fibers for Skin Regeneration” presents a new possible method for skin wound healing that would be cost affordable, while also possessing antimicrobial activity and enhanced cell growth.

CHAPTER II

LITERATURE REVIEW

Skin Regeneration

Skin regeneration is the ability of the skin tissue to repair itself from a wound. A wound is the disruption of any tissue due to mechanical/physical, or metabolism related injuries. A mechanical or physical wound is caused by penetration, a cut or a crush, this leads to complications like hemorrhage, infection and fracture. A metabolism related wound is one such as those caused by diabetes and other metabolic deficiencies. The healing of the skin wound is a complex but necessary process. Skin wound healing will lead to skin regeneration which is, as mentioned, a complex process that requires efforts of many factors and cell lineages. The process has distinct phases: proliferation, migration, matrix synthesis, presence of growth factors signals, and matrix signals. The overall healing process is still under research and effort is being made to further the understanding of the wound healing process. [1] Cell proliferation is the increasing of number of cells which is defined by the balance between cell division and cell death or cell differentiation. Cell migration is an orchestrated movement of cells in a certain direction to a specific location that is necessary for wound healing, embryonic development, and immune responses.

Burns

Burns are examples of physical and mechanical wounds. Burns are injuries caused by exposure to heat, friction, radiation, electricity, or chemicals. The American Burn Association reports that more than 450,000 patients receive hospital and emergency room treatments for burns each year [2]. From this 43% are from exposure to fire or flames, 34% for exposure to hot steam or liquid, 9% because of direct contact with a hot surface, 4% electrical, and 3% from chemical exposure [3]. Burns are characterized by degree, this is based on the severity and depth of the damage. First degree burns can be easily treated at home, while second and third degree burns often require specialized attention. This third degree burns often require surgery and skin grafts, which is when a surgeon removes skin from another part of the body and proceeds to use it as a scaffold in the affected area. Burn treatment requires daily cleanings, and aseptic conditions to keep the patient from infection from bacteria or viruses while also preventing loss of heat through the open wound [4].

Diabetes

The increase in diabetes diagnosis in the population is estimated to go up to 592 million among adults in the world. [5] Diabetes can be a precursor of metabolically related injuries. Diabetes is a condition where the production or response of the body to the hormone insulin is impaired. This results in an abnormal metabolism of carbohydrates and subsequently elevated levels of glucose in the blood stream. High glucose in the blood stream changes the rigidity of the cell walls, narrowing the blood vessels, hence promoting poor circulation, which decreases the delivery of nutrients and oxygen to the different parts of the body. Diabetics, therefore, have a slower wound healing process, 25% of diabetics are expected to develop foot ulcers. [6] With

progression of the wounds or slow healing of the wounds, diabetic's patients need special attention when they suffer a skin injury and an advancement on skin regeneration would benefit these patients. [7]

Skin

Tissue are a group of cells that are specialized to perform a specific function and together become an organ. The skin is the largest organ in our body. It has many functions that helps us live day to day. It's the first barrier of protection for the organism, it protects from microorganisms, radiation, toxic substances, among others. The skin also regulates body temperature, prevent loss of essential body fluids, and excretes toxic substances.

The skin is composed of three layers; epidermis, dermis and hypodermis. The epidermis is the outer layer of the skin and it prevents the entry of microorganisms and maintain body hydration. The epidermis is divided into five layers that are made of different immune and non-immune cells, such as keratinocytes, T cells, and stem cells, among others. The dermis layer is the layer located between the epidermis and the hypodermis, this layer is composed of collagen protein, blood and lymphatic vessels, sweat glands, nerve cells, and stem cells. The dermis provides structural toughness to the skin. The hypodermis is known as the subcutaneous fat its primary function is to give anchorage and support the dermis and epidermis. The hypodermis is composed of adipocytes, macrophages, nerves, vasculature and fibroblasts.

Wound Healing Process

As mentioned wound healing it is a multistep process. In normal conditions the process is achieved by four phases: homeostasis, inflammation, proliferation and remodeling. [8] If the biological pathways that control and activate these processes is interrupted or impaired the wound repair process would be affected and this could lead to a scar or non-functioning mass of fibrotic tissue [9].

In hemostasis, the initial phase begins as an autonomic response to attempt the minimization of damage. Platelet aggregation starts, the immune system activates, and the blood clotting process starts recruiting vitronectin, fibronectin, fibrin and thrombospondins, which start the scaffold like matrix for the migration of cells. [9] The second phase, inflammatory, can be divided into three phases or sub-phases where first the neutrophils arrive the first day, three days after the monocytes starts transforming to macrophages. During these three days of the inflammatory phase some factors starts to be produced, such as the tumor necrosis factor (TNF-α), interleukin 1 (IL-1) and interleukin 6 (IL-6). The inflammatory response stimulates the vascular endothelial growth factor (VEGF), interleukin 8 (IL-8) to stimulate the repair of vascular vessels, transforming growth factors (TGF-α and TGF-β), fibroblast growth factor (FGF), and platelet derived growth factor. [10-13] Following the inflammatory response, from approximately the third to the tenth day, the proliferation phase occurs. Reepithelization is induced by the activation of growth factors and cytokines, which cause the expansion of the keratinocytes, epithelial cells, stem cells and fibroblasts. [9, 13-14] In this phase, angiogenesis is induced. Angiogenesis is the creation or synthesis of new blood vessels that are used to transport biomolecules, factors and oxygen to the affected area. [15, 16] The ultimate step is the production of granulation tissue, which is made of fibroblasts, granulocytes and macrophages.

Fibroblasts are the main cells during the granulation, since they induce the production of collagen and other EMC molecules. The EMC provides a scaffold for cell adhesion and proliferation. In this last moments of the proliferation and granulation phase, the fibroblasts differentiate into myofibroblasts which, forms a scar, or they undergo apoptosis (cell death). [17]

Two to three weeks after the wound damage was made the last step of wound healing is known as the remodeling or maturation phase, which can last up to a year or more, depending on the severity of the wound. In this phase the tissue is realigning along the lines of stress. Also, unnecessary vessels formed during granulation are removed via apoptosis, finally a scar made of collagen, with a small number of fibroblasts is left. [9, 18-19]

Wound Therapy

Biological based wound healing approaches

Application of topical antimicrobial substances such as topical antibiotics is a conventional way of treating wounds, where the main objective is the reduction of the chances of infection and its complications by destroying the microorganisms that can cause said infection. Immune based antimicrobial molecules and therapeutic microorganisms are being investigated as possible treatments for wound healing as well. [20]

Antimicrobial peptides (AMPs) are immune based antimicrobial molecules that can be found naturally or synthesized. These molecules have specific amino acids that produces amphipathic conformations. Bacteria, and some animals such as amphibians, insects, and mammals produce AMPs, it is still under research the discovery of other organisms that may produce these peptides. [20, 21] AMPs have a broad spectrum of antibiotic activity against viruses, bacteria, yeast and fungi. Some AMPs have been found to neutralize endotoxins activity;

cathelicidins and defensins are two naturally occurring examples. [22] Cathelicidins and they derivatives peptides can be used to treat wound infections from burn related wounds. [22, 24] Furthermore, there are synthetically AMPs (S-AMPs) that are being synthetized and investigated for wound healing applications. Some examples of this laboratory synthesized AMPs are IK8D, IK8L, and IK8-2D that are S-AMPs that inhibit the resistance of some bacteria such as the gram-negative *P. aeruginosa*, the most common bacteria found in infected burn wounds. [25] Other S-AMPs, such as D-IK8 and WR12 were found to inhibit the MRSA (methicillin-resistant *Staphylococcus aureus*) in stationary and intracellular bacterial growth. [26]

Stem cell based wound therapy

Stem cell wound therapy employs the use of stem cells for wound healing. Stem cells are either extracted from a human or induced. Most studies use induced stem cells or pluripotent cells which are later induced to differentiate into specialized cells for the tissue needed.

Cell imprinted biomaterials mimic the natural environment for stem cells and induce stem cell differentiation and proliferation for wound healing and artificial tissue applications [27, 28] It has been reported that imprinted substrates, such as PDMS casting based-cell-imprinted micro/nano environments, functioned as artificial nanostructures for skin repair by inducing skin cell differentiation helping in cutaneous wound healing. [29]

Nanotechnology

Methodologies for better care in infectious burn wounds and topic wounds are necessary to maintain and promote faster and better skin regeneration. Nanotechnology has introduced a wide variety of materials for wound healing and skin regeneration that comprises different

morphologies in the sizes of 1nm to 1000nm. [30-32] Within nanotechnology organic nanoparticles (NPs) and inorganic NPs will be discussed. NPs are usually used to deliver drugs to relieve pain, and act as antimicrobials. Organic NPs are usually synthetized by self-assembly, the most common materials used are chitosan (CS), Poly (lactic-co-glycolic acid) (PLGA), dendrimers and hydrogels. [33]

CS can be used as a natural and biodegradable substance in the design of drug delivery systems. CS is a cationic polymer that provides antimicrobial properties, preventing microbial infections in a topical wound [34-36], as a prophylactic CS reduces the spreading of infection and accelerates the wound healing process. [37, 38] Studies have found that CS NPs helps the wound healing process by facilitating the growth of fibroblasts and osteoblasts, also CS NPs increases the wound's inflammatory function [33, 34]. CS is used as a component in a many wound dressings [39].

PLGA is a biocompatible, biodegradable, non-toxic, US Food and Drug Administration (FDA) approved material that is often synthesized be the emulsification of hydrophobic components in an organic solvent. [40] PLGA NPs promotes wound healing, also it has been studied that PLGA increased fibroblast proliferation rate thus accelerating wound healing. [41] Studies reveal that PLGA with incorporated LL37, which is an endogenous human defense peptide that modulates wound healing and has antimicrobial activity, accelerates wound healing and acts as an effective antimicrobial agent in infected wounds. [42, 43]

In another study, dendrimers are used. This is a nano-scale polymeric macromolecule that have a monodisperse and homogeneous structure, with antibacterial property. Dendrimers help destroy bacteria by disrupting the cell walls of the bacteria because of its positively charged groups reacting with the negatively charges groups within the bacterial wall. [44, 45]

One of the widely discussed and researched wound healing methods are the hydrogels. These materials are hydrophilic 3D structures made from polymeric networks which can absorb substantial amounts of liquid. [46] Due to its high porosity and soft consistency they are suited to be used as dressings in wound healing and skin regeneration. Hydrogels can protect the wounded tissue while providing comfort to the patient with an ECM-like structure that allows better cell growth compared to a 2D substrate. Studies show that hydrogels can be optimized to reduce scars (be antifibrotic) and to have antimicrobial activity which helps in wound healing and skin regeneration in burns and diabetic patients [47]. Hydrogels have other features that makes them a desired material among researchers for wound healing and skin regeneration. Hydrogels can be modulated to carry and release various bioactive molecules such as growth factors and antimicrobial agents that assist in wound healing and in the implementation of exogenous cells such as fibroblasts, stem cells or epithelial cell encouraging faster and better proliferation of cell during wound healing. [48] In another study, compatible hydrogels were designed using chitosan and encapsulating clarithromycin, with ability to be administered topically, suggesting being promoting wound healing and skin regeneration. [49] Also, some researchers suggest that stem cell loaded hydrogels increase vascularization thus promoting wound healing. [50]

Furthermore, quantum dots (QT), metallic NPs, and carbon-based NP have been used for burn wound healing as drug delivery systems and as antimicrobials. Studies have revealed that gold NPs (AuNPs) were used to culture cryopreserved human fibroblast cells can facilitate skin repair and improve collagen production of third degree burns in white male rats. [51] AuNPs/Collagen scaffolds were designed and crosslinked with glutaraldehyde which had good biocompatibility, high mechanical strength, and stability against enzyme degradation while producing neovascularization and improving wound closure. [52] Silver NPs have also been used

in research for burn wound treatment. A few recent studies found that Ag-containing hydrogels were a non-cytotoxic alternative to use for healing of burn wound infections when compared to the commercial and most used alternative, silver (Ag) nitrate. [53] AgNPs also showed no cytotoxicity and were localized in the cytoplasm of fibroblasts, in vivo and in vitro studies of full thickness skin damage. [54] As mentioned, the wound healing is an orchestrated and highly organized process that requires specific factors and cell lineages, in the excess of any, the process might be disrupted, in this study AgNPs were also used to decrease the over inflammatory response by decreasing the secretion of VEGF and pro-inflammatory cytokines, therefore promoting a better healing. [55] Other studies show that a combination of graphene QDs and AgNPs was found to have antibacterial properties against *S. aureus* and *P. aeruginosa*. [56] On the other hand, some metallic NPs, such as copper (Cu) NPs were found to have a broad spectrum of antimicrobial activity against yeasts, viruses and bacteria, however CuNPs can be very toxic to the cells, CuNPs can denaturalize or damage proteins and can cause some rapid oxidation reactions in unsaturated lipids, hence being toxic to the tissues and cells. [57] Innovation in nanotechnology have helped in a way that Cu antimicrobial activity can be taken advantage while minimizing its side effects. A study where Cu was encapsulated in CS NPs was successful in delivering a synergistic activity between the two while having a successful antimicrobial activity. [58] As with metallic NPs, carbon-based NPs have been found to have antibacterial properties. In one study Cu/Zn bimetallic NPs combined with carbon Nano fibers (CNF) were found to suppress the growth of *E. coli* and *MRSA*. [59] Another study found that singled wall carbon nanotubes (SWCNTs) caused the death of microorganisms, furthermore fullerenes have also shown intrinsic antimicrobial activity against different bacterial species. [60]

Scaffolds research is an active topic for wound healing. Among these, there are 3D bio-printed scaffolds, engineered films, hi-tech wound dressings and nanofiber scaffolds, and a combination of the previously mentioned therapies incorporated into scaffolds.

3D bio-printed scaffolds, a progressing technology, is an advance technology that is fast developing where complex biomolecules, proteins and even cell can be patterned or designed by computer software and manufacturing tools such as CAD and CAM, and later printed using layer-by-layer deposition. [61] One study produced eight human-like skin collagen layers. It consisted of implanted cells within the collagen layers which was constructed in poly-d-lysine coated glass petri dishes. [62] Further studies have conducted to the utilization of smart materials for 3D bio-printed scaffolds which allow the material's shape, performance and properties to change over time or to change because of a stimulus, known as 4D bio-printed. [63] Studies of the 4D materials for bone and other vessel regeneration suggest that they could be the next generation of materials for other organs regeneration such as skin. [64, 65] An example of this smart materials is dimethylaminoethyl methacrylate (DMAEMA)/hydroxyethyl methacrylate (HEMA) scaffolds that upon pH stimuli or change in pH can control the transport or molecules and migration of cells into the scaffold. This study showed improvement in the formation of granulated tissue in the pH dependent scaffold when compared to a non-pH sensitive scaffold. [66] Another pH dependent study shows the controlled release of tannic acid (TA) in acidic and swelling environment. [67] TA is a specific form of tannin that have antioxidant, antimicrobial and anti-inflammatory properties [68-70] This studied exhibited that at constant release of TA good antibacterial effects was obtained while no toxicity to 3T3 fibroblasts were reported. [67]

Fibers are another hot topic among tissue regeneration research. Fibers are obtained from different methods, however, for tissue regeneration, fibers are mostly developed by electrospinning. Electrospinning is a technique that uses high electric force draw charged polymer threads hence extruding polymer fibers out of a spinneret with polymer solution or polymer melt forming fibers of small diameter (micro to nanometers in diameter). [71]

One study found that Dimethyloxalylglycine (DMOG) loaded PCL/Col nanofibrous wound dressings facilitated diabetic wound healing by providing an environment for cell growth and inhibiting hypoxia in the patients. [71] Another study demonstrated how an antibiotic, cefazolin, could be incorporated into PLGA fibers. [72] A study of a mixture of PVA, PVAc and the antibiotic ciprofloxacin HCl showed release of the antibiotic over 250 hours. Results showed lowering the degree of swelling of the wound while the antibiotic was being released. [73] Electro-spun PVA and sodium alginate was evaluated in vivo for wound healing where the findings show that the performance in wound healing increased after the 21st day compared to the commercially available wound dressings tulle grass. [74] Another study shows enhancement in skin cell migration when growing in PLLA nanofibers furthermore other studies confirm epithelial cell migration from the wound edges throughout fibers. [75-76] Other polymer and composites have been studied such as poly D, L-lactic (PDLLA)-poly ethylene oxide (PEO) nanofibers loaded with the iron chelator DHBA, PDLLA-PEO nanofibers containing Cu, silk fibroin/PLGA nanofibers which demonstrated to have therapeutic properties against bacteria and provide a ECM-like environment to accelerate the wound healing process. [77-79]

A new way of obtaining fibers for wound healing is through the Forcespinning® technology. Forcespinning® is capable of producing nano and micro fibers depending on the chosen parameters. When compared to electrospinning the yield or amount of fibers per polymer melt or polymer solution is greater, thus making commercialization easier. Forcespinning® is further discussed in chapter three. There has been some research of fibers for skin wound healing using Forcespinning®.

One example is a study on composites of PVA/CH/TA where the authors successfully spun fibers and report improvement in cell growth and proliferation while exhibiting good antibacterial activity. [80] A similar study uses CH/PL/TA, having similar findings: good antibacterial properties and excellent cell proliferation throughout the fiber mat. [81] Other fibers, such as cellulose embedded with silver nanoparticles have been developed by Forcespinning® and have been proved to have great antibacterial properties, and water absorption suggesting that they could be potentially be used for wound healing [82]. Another, research demonstrate that Gelatin/poly (epichlorohydrin-co-ethylene oxide) (GL/PECO) composite fibers were successfully developed by Forcespinning®. GL/PECO fibers demonstrated to have good drug release properties over a fifteen-day experiment and excellent cell viability was observed for NIH/3T3 fibroblast cells. [83]

Even with the extensive research focused on wound healing and skin regeneration, there is no practical solution to address this issue. This thesis focuses on studying polymeric fibers membranes developed through Forcespinning® for possible in-situ application for skin wound healing.

One of the polymers studied here is polyhydroxy butyrate (PHB). PHB is a semi-crystalline biopolymer that is produced by microorganisms and belongs to the polyesters group.

PHB is of great interest for application in bone tissue regeneration and implants, it sinks in water, have good oxygen permeability and is non-toxic however the polymer only dissolve in some organic solvents such as chloroform and other hydrocarbons. One study suggests that chitosan/PHB fibers prepared by electrospinning promotes fibroblast cell attachment and proliferation. [84-85]

Polyvinyl butyral (PVB) is also studied here. PVB is a polymer which applications range from adhesives to food packaging. PVB is a highly hydrophobic polymer that contains some hydroxyl groups. As more hydroxyl groups present in the polymer less hydrophobic the polymer become. One study shows that PVB can be spun into fibers by electrospinning and can uptake additives such as antibiotics and nanoparticles increasing the antibacterial properties of the material. [86] One patent shows mammalian cell growth in a medium free PVB surface [87] suggesting PVB as a possible material for cell growth hence wound healing.

Polylysine was used in the development of the polymer fibrous membranes. It is commonly used to induce cell adhesion in cell culture surfaces by facilitating cells adhesion and growth in solid surfaces, such as in cell culture plates. Polylysine enhances electrostatic interaction between negatively charged ions of the cell membrane and positively charged surface ions of attachment factors on the culture surface increasing the number of positively charged sites in the surface available for cell binding thus inducing better cell adhesion. [88, 89]

As a summary of the literature review, skin wound healing can be addressed by reducing infection risk and by providing an environment that supports cell growth and proliferation. The cells need a matrix where they can attach and proliferate and keep sending biochemical signals until the wound process is completed resulting in a healthy tissue. The ECM is composed by different fibers, cells, blood vessels and molecules that play important roles in wound healing.

Tissues are composed by cells, which is the basic structure of life. In this project, NIH 3T3 Mouse Embryonic Fibroblast cells were used. Fibroblast cells are present in a normal wound healing process. They secrete molecules that are the precursor of the collagen, which is one of the main fibers that compose the ECM.

Skin grafts are the technology most widely used in hospitals to treat burns and wound healing for third degree burns, skin infections, or large and deep wounds, though still this process is not cost effective (actually synthetic skin grafts are mostly cost prohibitive). By using polymers fibers in-situ, risk of infection could be reduced as well as treatment cost. This thesis studies the possibility of using polymer fibers for an in-situ application for skin wound healing.

CHAPTER III

MACHINES, EQUIPMENTS AND TOOLS

Scanning Electron Microscopy (SEM)

Scanning electron microscopy or SEM is a technique that provides high resolution images. It is an electron microscopic technique that uses a beam of electrons to produce high resolution imaging of the surfaces of a sample. [90] As a light microscope uses visible light to visualize a sample, the SEM uses an electron beam that gives the advantage of going into higher magnification (over 100,000X) and greater depth of field (up to 100 times more than light microscopy). In SEM the electrons interact with the atoms of the sample producing a variety of signals that contain information of the sample's morphology or topography, and composition and is later detected by specific detectors and a computerized image is produced by the beam's position combined with the detected signal. [90, 91]

The SEM works in both high vacuum and low vacuum, known as conventional SEM and variable pressure or environmental SEM respectively. [91]

The SEM is composed by various parts as shown in Figure 2. The upper portion of the microscope is where the electrons are being generated, known as the electron source. The electrons are generated by thermal emission, most SEM use a tungsten filament that have about 100 nm of radius, this filament heats up creating a cloud of electrons, or the electrons are

generated by a field emission cathode. [90-93] (The way it works is by creating a high potential gradient between the electrodes causing a field electron emission)

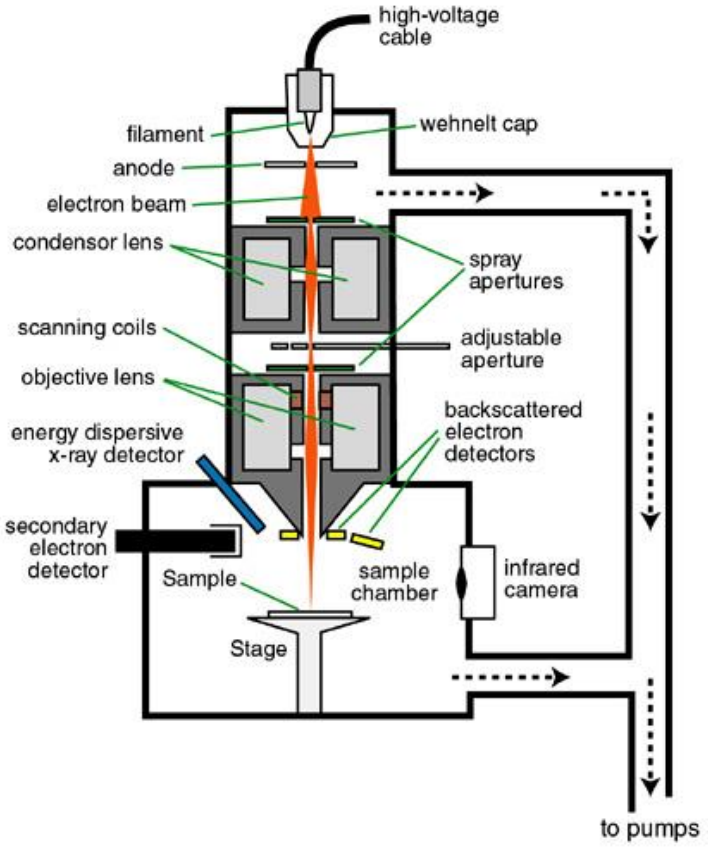

Figure 2. Scanning Electron Microscope Schematic. [92]

The thermal emission source will release electrons in an electron column and are further aligned with a series of electromagnetic lenses. The energy of the electron beam can range from 100eV to 30kV depending on the model of the SEM and the evaluation objectives. [91, 93] While it's rare for an SEM to have detectors for all the possible signals, the SEM have the ability of incorporating various detectors that can detect and make an image from different interactions of the electron beam with the atoms of the sample. The different electron-sample interactions

include secondary electrons (SE), back scattered electrons (BSE), characteristic X-rays, cathodoluminescence, absorbed and transmitted electrons shown in Figure 3. [91-92, 94]

The most common SEM detector used is for secondary electrons which is standard for all SEMs. The secondary electrons are emitted from the surface of the specimen or sample. The secondary electrons are generated as ionization product when the electron beam energy exceeds the ionization potential the beam electron interact with the atom releasing a secondary electron from the surface which is detected, and a high-resolution image is created revealing details as little as 1nm in size. [95]

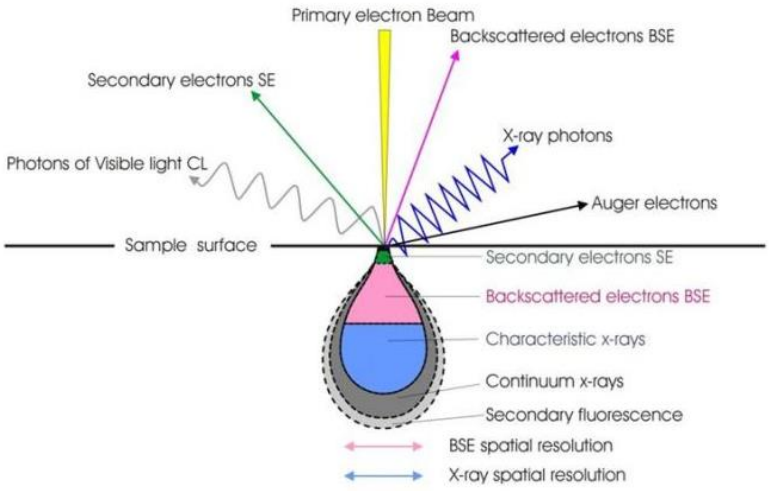

Figure 3. Different electron signals. [91]

The back scattered electrons are the electrons from the electron beam that are reflected or backscattered from the sample by elastic scattering. These images are of less resolution than the SE because of the nature of the electron-sample interaction which, is an elastic scattering interaction between the electrons and the atom, the same electrons from that electron beam that interacts with the sample are the ones being reflected. [91-92, 94, 96]

Characteristics x-rays are produced when the electron beam removes an inner shell electron from the sample causing a higher energy electron to move to fill the void releasing energy in the process. These are usually used to identify the composition of the material of the sample. [91-92, 94]

Cathodoluminescence happens when electrons impacting on a luminescent material cause the emission of photons which may have wavelengths in the visible spectrum. This describe the absorbed electrons as well that emits a photon of electromagnetic energy. [91-92, 94]

The SEM essential components include an electron source, electron lenses, a sample stage, detectors for the signals of interest, a display or data output device such as a computer, and to comply with its infrastructure requirements, such as a power supply, a vacuum system, a cooling system and a vibration-free floor or table. [90-91]

The electron source or electron gun provides a steady electron supply for the electron beam, which is aligned, first by letting the electrons go through a small aperture, and then using different electron lenses. As shown in Figure 4 the SEM usually has three or more pair of electron lenses: the first condenser lenses and second condenser lenses help align the beam to a spot up to 5nm in diameter. The beam then passes through the scanning coils or deflector plates in the electron column, then using final or objective lenses the beam is deflected in the x and y axes in a scanning and raster manner in a rectangular area over the surface of the sample. The electron beam then interacts with the atoms of the sample creating a series of signals: secondary

electrons (SE), back scattered electrons (BSE), characteristic X-rays, cathodoluminescence, absorbed and transmitted electrons. [91-93]

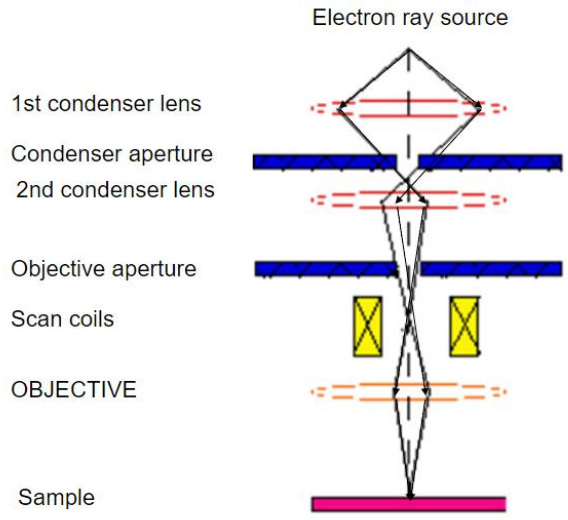

Figure 4. Electron beam alignment through apertures, lenses and coils. [94]

Most SEMs have an energy dispersive spectrometer (EDS) configured or installed (Figure 5). EDS uses the unique specific X-ray energy emitted by an atom to make a qualitative chemical composition analysis, to acquire elemental maps or spot analyses. [97]

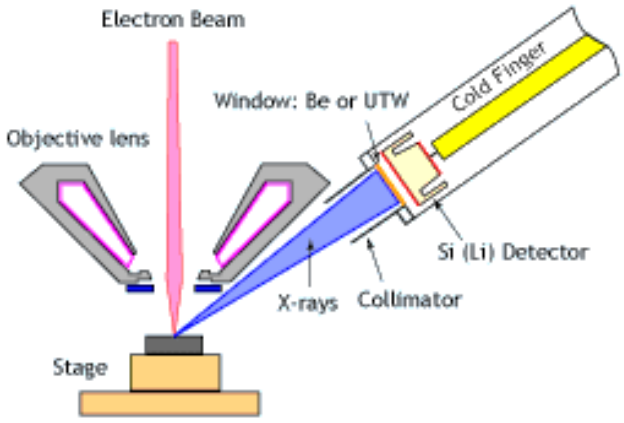

Figure 5. Schematic of an energy dispersive spectrometer. [97]

SEM is an essential instrument used for rapid characterization of solids materials morphology and topography, even elemental analysis is possible with an EDS addition to the instrument, however the SEM has some limitations, it does not support liquid samples and only support small samples (which dimensions rarely exceeds 40mm, the samples must be stable on vacuum conditions (on the order of 10^{-5} to 10^{-6} torr). Samples that are considered wet samples such as organic materials, swelling clays, and samples that are unsuitable for examination in a conventional SEM can be studied using a low vacuum or environmental SEM. [98]

Thermogravimetric Analysis (TGA)

Thermogravimetric analysis (TGA) is a method used for thermal analysis in which the mass of a sample is measured over time as a function of temperature which is increased at a constant rate. TGA provides information or data about the physical phenomena of the material such as phase transitions, absorption and desorption.

There are three types of thermogravimetry: dynamic, isothermal or static, and quasistatic. Dynamic TGA is the type of analysis where the sample is subject to constant increase in temperature. Isothermal TGA is the analysis made when the sample's weight is recorded while at a constant temperature for a period. Quasistatic TGA is the analysis where the sample is heated to maintain a constant weight loss. [99-101]

TGA as shown in Figure 6, consist of a sample pan supported by a precision balance which are inside a furnace and is heated or cooled during experimentation while the mass of the sample is being monitored. The environment inside de furnace is controlled by a sample purge gas which may be inert or reactive that flows through the sample and exist the furnace through an exhaust. TGA can quantify loss of water, solvent plasticizer, decarboxylation, pyrolysis,

oxidation, decomposition, weight percent filler, amount of residue remaining after the rest of the material is degraded. [99]

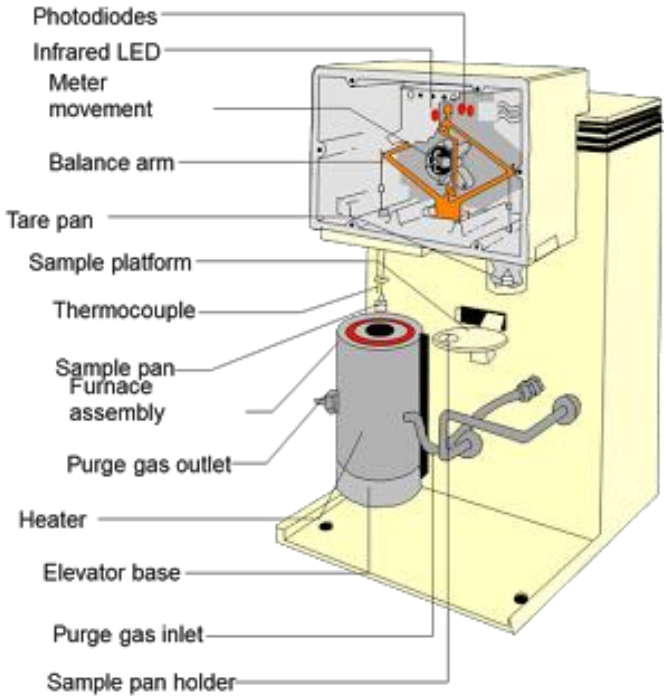

Figure 6. Schematic of a thermogravimetric analyzer. [99]

TGA can measure thermal stability of the material, oxidative stability of the materials, composition of multi-component systems (such as composite, fillers, etc), estimated lifetime of a product, decomposition kinetics of the materials and the effect of reactive or corrosive environments and moisture and volatile contents of the materials.

TGA is used to characterize polymeric materials such as thermoplastics, thermosets, elastomers, composites, films, fibers, coatings, and paints, through the analysis of the decomposition patterns. [100-101] TGA use a precision programmed balance for increase in temperature known as thermobalance. The results are often displayed as mass percentage vs temperature or time these curves are known as thermogravimetric curves. [101]

The first derivative of the TGA curve (the DTG curve) may be plotted to determine inflection points useful for in-depth interpretations as well as differential thermal analysis.

Differential Scanning Calorimetry (DSC)

The differential scanning calorimetry or DSC is a characterization method used to measure the heat flow associated with the transitions in a material. Calorimetry is the science that study the measure of heat exchange of chemical reactions or physical events. All chemical and physical reactions involve energy, or an exchange of energy with its surroundings, either exothermic or endothermic. DSC measures the amount of energy in the form of heat or temperature to go from one state to the other in a cycle manner. [102]

As shown in Figure 7 DSC works using two pans, one containing the sample and an empty pan, known as reference pan. Both pans are heated at a constant rate and the temperature is constant for both pans. DSC measures the difference in heat flow needed when the material undergoes a physical transformation such as an endothermic transition like melting which requires more heat flowing to the sample or an exothermic transition such as crystallization which requires a heat flow from the sample to its surroundings. [102,103]

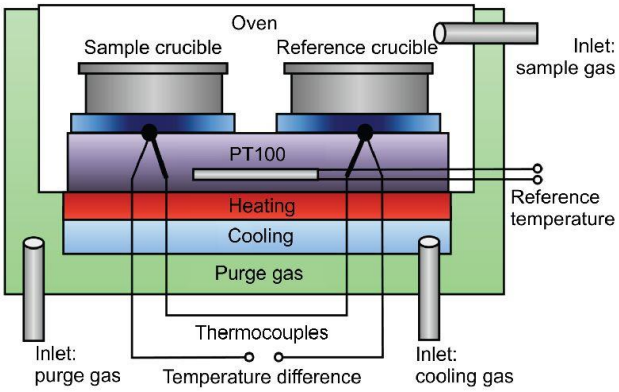

Figure 7. Schematic of a differential scanning calorimeter [102]

The pans are placed over a constantan disc on top of a platform inside the DSC cell with a wafer (thin slice of semiconductor material) underneath. The heat flow is measured by measuring the temperatures across the sample and reference wafer using a thermocouple that is located under the constantan. This test can be done under air or under a controlled environment such as having an inert gas constant purge into the DSC cell, it can also be done under vacuum and controlled mixed gases. [102,103]

Forcespinning®

Forcespinning® is a process that uses centrifugal force to make micro-scale and nano-scale fibers. [104] Forcespinning® uses a polymer melt or polymer solution that is placed inside a spinneret and forced out through small orifices using centrifugal force caused by angular velocity of the spinneret. The material is jetted in to the air and made into fibers through inertial shear forces. Forcespinning® variables are the rotational speed of the spinneret, orifice diameter and configuration of the needles attached to the spinneret, spinneret aerodynamics, polymer melt or solution viscosity and distance from the spinneret to the collectors. [104,105]

As shown in Figure 8 Forcespinning® uses a motor that rotates and spin the spinneret which contains the polymer melt or polymer solution. Then the polymer is forced out of the spinneret through small orifices, causing the elongation of the polymer to make fibers. It usually works with medium to high molecular weight polymers because the entanglement between the polymer chains is key to help build the polymer fibers. Forcespinning® machine is enclosed in a chamber with doors to access the spinneret, collectors and fibers. Inside the chamber there is a heater and oven to melt the polymer melt in the spinneret, when using a polymer solution, it is often done at room temperature. The fibers are collected in a crown like collector or using a

series of single collectors arranged in a round manner around the spinneret. The final collection of the fibers is done by using a frame collector and collecting by hand or a vacuum collector. [105,106]

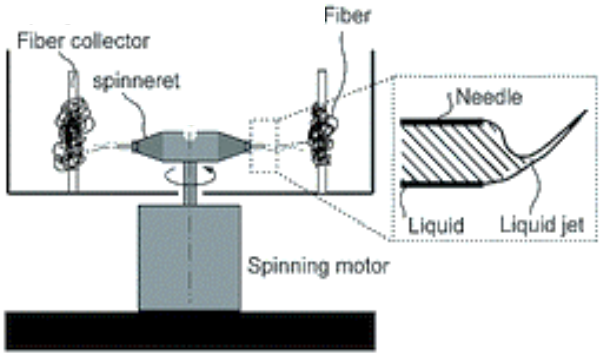

Figure 8. Schematic diagram of Forcespinning®. [106]

Biosafety Cabinet

A biosafety cabinet is an enclosed and ventilated laboratory workspace. This space is usually used to work with contaminated or potentially contaminated materials or used to work with materials that need an extra clean workspace such as cell cultures. They are divided into biosafety levels, differentiated by the degree of the containment required for the job. All classes provide personal protection, from class II and class III provides materials protection as well. [107-108]

The safety cabinets operate using a motor driven fans mounted in the cabinet which draw directional mass airflow around the user into the air grille as shown in Figure 9. The air flows from underneath the work surface and back up to the top of the cabinet where is passes through a high efficiency particulate air (HEPA) filters. The air entering the cabinet comes from a filter system that is a column of HEPA filtered, sterile air which maintain the work area sterile.

Depending on the type of class of the biosafety cabinet the air is recirculated into the laboratory or exhausted through an HEPA filter on to the atmosphere through an exhaust system. [109]

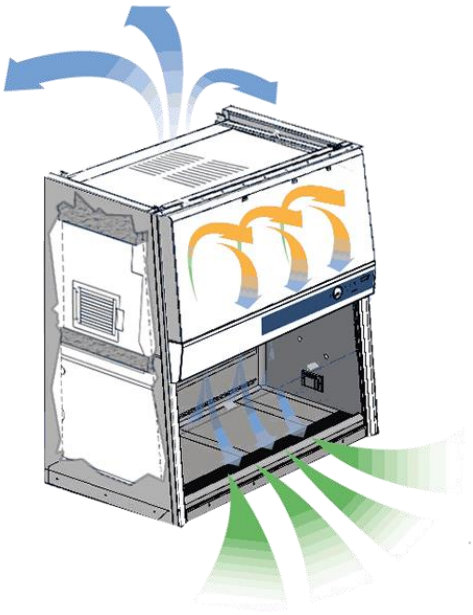

Figure 9. Schematic of Biosafety Cabinet [109]

The inflow and outflow vary by model, brand and type of the biosafety cabinet. A Ultra-Violet (UV) lamp often comes in the biosafety cabinet to help decontaminate the surface of the workspace before and after the experiments are done and it is regularly used before the experiments to assure a decontaminated surface. [107-108]

Confocal Microscopy

Works by passing a laser beam though a light source aperture which is then focused by objective lenses into a small area on the surface of the sample, this beam scan the sample and an image is built up pixel by pixel by collecting the emitting photons from the fluorophores in the sample.

The confocal microscope focuses by using point illumination and a pinhole that are placed in front or the detector, hence the name confocal. The only light that can be detected is the fluorescence produced close to the focal plane creating a great resolution image among all the fluorescence microscopes. [110]

Figure 10 shows a schematic of the confocal microscope and how the laser travels through the microscope until it reaches the detector. The laser excitation source emits a laser that goes through a pinhole aperture and then the beam is reflected in a dichromatic mirror and goes through the objectives to the specimen from there the specimen emits fluorescence, and only the in-focus emission goes though the detector pinhole aperture and the detector reads the signal which is sent to a computer where an image is built pixel by pixel. Most confocal microscopes build the images 3 pixels per second depending on how many pixels per image. [111]

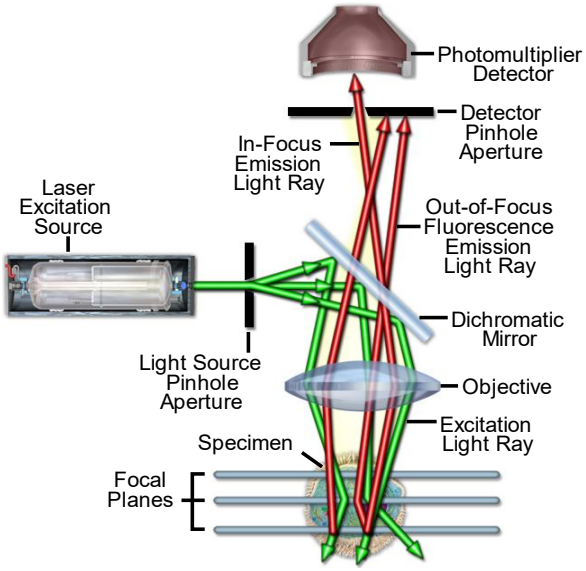

Figure 10. Schematic of a Confocal Microscope [110]

Hotplate

The hotplate or magnetic stirring is used to heat up a solution or sample and stir using a magnet. The magnetic stirring hot plate usually have an on/off switch, temperature and speed knobs or bottoms, a ceramic table or plate that resist elevated temperatures and a temperature resistance and corrosion resistant shell.

A heating element is usually incorporated to the stirrer to allow the plate to heat when heat and stirring are needed in a reaction. The power range for the heating element can range from a few hundred to a few thousand watts and can be controlled by the user to reach a desired temperature. It works is either by a magnetic field created by a rotating magnet or by a set of stationary electromagnets that makes the stirrer on top of the plate to rotate. [112]

Incubator

An incubator in biology is used as a device that provides the environment needed for cells or organism to grow in a laboratory setting. The incubator maintains optimum parameters for the growth of cells such as temperature, Carbon Dioxide (CO_2) levels, and humidity. Most incubators used for cell growth in most laboratory settings as shown in Figure 11 have different shelves, CO_2 inflow, a water bath in the lowest shelf and a thermostat. Some incubators are made of copper and others of alloys that help maintain aseptic surfaces and a constant temperature. [113]

Figure 11. Biological Incubator. [113]

Figure 12 depicts a schematic of an incubator, where there is an inflow and outflow of a gas, usually CO_2, a control unit that controls the temperature and a water bath that with the control unit control the humidity of the incubator. It is important that for the incubators with only one source of heat, to have air circulation to maintain uniformity of temperature and gases inside the chamber; however there are incubators with heat sources all over it surfaces that also uses the airflow to maintain a homogeneous mixture of gasses inside it. [114]

The setup varies from incubator to incubator. For incubators that are going to be used to grow cells there is usually a water bath that is heated by the same chamber temperature which is usually set to 37 °C and a concentration of CO_2 and O_2. There are also incubators that provides different chambers where the researcher can control its parameters for different concentration of gases and temperatures.

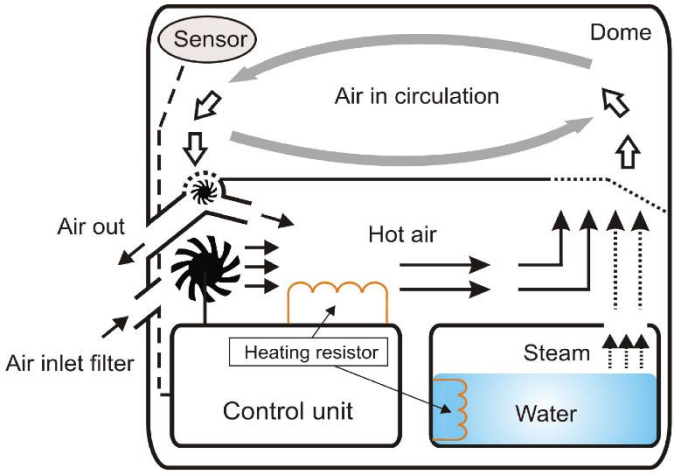

Figure 12. Schematic of a Biology Incubator [114]

Contact Angle Meter

Contact Angle Meter allows you to measure the contact angle between a sample surface and a liquid or the wettability of the surface of a solid by a liquid. Using a camera and a light a shadow of the liquid is created, which is deposited in the surface of the sample and then photographed by the camera and recorded in the computer. This angle measurements are automatically made by the computer or when the computer doesn't automatically recognize the drop the program allows you to modify the angle measured by placing the arrows/angle where it is supposed to be and measuring the angle between the droplet and the surface. [115]

CHAPTER IV

MATERIALS AND METHODOLOGY

Materials

Medium–molecular weight Chitosan (MW=50,000–190,000 g/mol and 75%–85% degree of deacetylation), Tannic Acid (from Chinese natural gall nuts), and Citric Acid were purchased from Sigma–Aldrich (St Louis, USA). The bath sonicator was purchased from Fisher Scientific (Pittsburgh, USA). Deionized (DI) water (18MΩcm) was produced from Mill-Q (Millipore Ltd, Hertfordshire, UK).

Polyhydroxy butyrate (PHB) (MW=55 0,000 g/mol) was purchased from Goodfellow Cambridge Limited (Huntingdon, England). Pullulan was purchased from Tokyo Chemical Industry CO., LTD. (TCI America, Portland, OR)

Poly (vinyl butyrate) (PVB) 60H (18-21wt% -OH, and 1-4wt% Acetate) about 70-80% Butyral (Houston, TX) and PVB 60T (24-27wt% -OH, and 1-4wt% Acetate) about 70-80% Butyral (Houston, TX) were used as purchased. Ethanol Anhydrous was purchased from Fischer Chemical (Fischer Scientific, Fair Lawn, NJ, USA).

Poly-D-lysine hydrobromide (MW=30,000-70,000 g/mol) was purchased from Sigma Aldrich (St. Louis, USA). Poly-D-lysine was dissolved in water as per instructions from Sigma

Aldrich and modified with chloroform and ethanol (poly-D-lysine will be called polylysine for the rest of the thesis):

1. H_2O with polylysine: polylysine was dissolved in 50mL of water.
2. Chloroform with polylysine: polylysine was suspended in 50 mL of chloroform.
3. EtOH with polylysine: polylysine was suspended in 50 mL of ethanol.

70% denatured ethyl alcohol was purchased from Fischer Scientific (Pittsburg, PA, USA) 10X Phosphate Buffered Saline (PBS) was purchased from Fischer Scientific (Hampton, NH, USA) and diluted to 1X PBS using DI water. Mito Tracker (MTR) and DAPI was purchased from Thermo Scientific (Germany) and used as purchased. Formaldehyde, 16% (MW=30) was purchased from TED PELLA, Inc. (Redding, CA, USA) and was further diluted to 4% formaldehyde using 1X PBS.

Preparation of Solutions for Forcespinning® (FS)

Chitosan/Pullulan/Tannic Acid

1-3% Citric acid is added to dH2O, once its dissolved 3% Chitosan was added and waited over night to dissolve or 2-3 hours at 75°C in constant stirring to dissolve, then 18% Pullulan was added and dissolved overnight in constant stirring, once dissolved 1% TA was added to the solution, dissolved overnight. The solution was sonicated for an hour before spinning.

Chitosan/Pullulan/Tannic Acid/Polylysine

1-3% Citric acid is added to dH2O with poly-l-lysine, once its dissolved 3% Chitosan was added and waited over night to dissolve or 2-3 hours at 75°C in constant stirring to dissolve, then 18% Pullulan was added and dissolved overnight in constant stirring, once dissolved 1% TA was

added to the solution, dissolved overnight. The solution was sonicated for an hour before spinning.

PVB

The 15% (w/w) PVB Solution was prepared by dissolving PVB in ethanol (EtOH) at 65°C to 75°C in constant stirring for 30 - 45 minutes. After cooling to room temperature, the solution was spun.

PVB/Polylysine

The 15% (w/w) PVB Solution was prepared by dissolving PVB in ethanol with polylysine at 65°C to 75°C in constant stirring for 30 - 45 minutes. After cooling to room temperature, the solution was spun.

PVB/Tannic Acid/Polylysine

The 15% (w/w) PVB Solution was prepared by dissolving 15% w/w PVB with 1% 9 (w/w) tannic acid in ethanol with polylysine at 65°C to 75°C in constant stirring for 30 - 45 minutes. After cooling to room temperature, the solution was spun.

PHB

For the 9% (w/w) PHB solution, PHB was dissolved in chloroform at 55°C to 58°C in constant stirring using two stirrers per vial for 4 - 4.5 hours at 58°C or overnight at lower temperature 55°C.

PHB/Polylysine

For the 9% (w/w) PHB solution, PHB was dissolved in chloroform with polylysine at 55°C to 58°C in constant stirring using two stirrers per vial for 4 - 4.5 hours at 58°C or overnight at lower temperature 55°C.

PHB/Tannic Acid/Polylysine

For the 9% (w/w) PHB solution, 9% (w/w) PHB and 1% (w/w) of tannic acid was dissolved in chloroform with polylysine at 55°C to 58°C in constant stirring using two stirrers per vial for 4 - 4.5 hours at 58°C or overnight at lower temperature 55°C.

For an easy referral the names of the samples and their respective contents are resumed in Table 1.

Table 1. Summary of Sample Names and Their Contents

Sample Name	Polymer	Additive 1	Additive 2	Additive 3
PVB	PVB			
PVB/Polylysine	PVB			Polylysine
PVB/TA/Polylysine	PVB		Tannic Acid	Polylysine
PHB	PHB			
PHB/Polylysine	PHB			Polylysine
PHB/TA/Polylysine	PHB		Tannic Acid	Polylysine
CH/PL/TA	Pullulan	Chitosan	Tannic Acid	
CH/PL/TA/Polylysine	Pullulan	Chitosan	Tannic Acid	Polylysine

Forcespinning® (FS) Process

Forcespinning® process requires a prepared polymer solution: PVB, PVB with polylysine, PHB, PHB with polylysine, CH/PL/TA, and CH/PL/TA with polylysine as discussed before. The solution is introduced into a spinneret using a syringe and an 18 ½ G needle. A 30 G needle will be placed in the spinneret, lock the doors, input the settings for the polymer solution as shown in Table 2.

Table 2. Cyclone Settings for the Different Samples

Material	Rotatory speed (RPM)	Time (minutes)	Collector distance
CH/PL/TA & CH/PL/TA/Polylysine	8000	8	Columns – 18-20 cm from spinneret
PVB, PVB/Polylysine & PVB/TA/Polylysine	6500	5	Columns – 14-18 cm from spinneret
PHB, PHB/TA & PHB/TA/Polylysine	6500	2	Columns - 18 cm from spinneret

CH/PL/TA & CH/PL/TA/Polylysine fibers were heat treated after spinning at 170°C for 4 hours to induce crosslinking. This helped the fibers to avoid dissolving in water.

Characterization of the Fibers

Scanning Electron Microscopy.

The morphology of the fibers was observed under a scanning electron microscope (SEM; SIGMA VP; Carl Zeiss, Jena, Germany). The average diameter of the fibers was measured using the image analysis software (Put software here) by randomly measuring 100 different points from the SEM images.

Thermal Analyses.

The thermo-physical properties of the fibers were analyzed by differential scanning calorimetry (DSC) and thermogavimetric analysis (TGA). DSC and TGA were carried out using the TA Thermal Analysis Instruments.

For the TGA the sample was weighted between 5-10 mg. The pan is tared inside the furnace, once is tared the sample was placed in the pan. The furnace was closed and the TGA was run from room temperature (RT) up to 800°C at a rate of 10°C/min. The sample for the DSC was prepared by weighting 5-10 mg of the sample and putting them in a hermetic pan with a hermetic lid. The DSC was set to run two cycles at 10°C /min from RT to the specified temperature and back to 30°C, twice and all the data was recorded by the computer. The settings for the DSC and TGA are showed in Table 3.

Table 3. DSC and TGA Temperature Setting

Material	DSC - Temperature Range- Cyclic (°C)	TGA - Temperature Range (°C)
CH/PL/TA & CH/PL/TA/Polylysine	25 to 200 (heating) 200 to 25 (cooling)	40 to 700
PVB, PVB/Polylysine & PVB/TA/Polylysine	25 to 250 (heating) 250 to 25 (cooling)	40 to 700
PHB, PHB/TA & PHB/TA/Polylysine	25 to 200 (heating) 200 to 25 (cooling)	40 to 700

Contact Angle Meter

Samples were prepared by cutting a 1cm x 10 cm fiber mat and placing it on a slide. The Contact Angle Meter DropMaster was turned on and the sample was placed in position. A 3µL water drop was placed on the sample and a picture was taken and the contact angle was measured. 10 drops were placed in each sample and 10 pictures were taken of each drop and the contact angle of each picture was measured, averaged and the data was analyzed.

Cell Culture

NIH 3T3 mouse embryonic fibroblast cells were cultured in a Dulbecco's modified Eagle's medium (DMEM) supplemented with 10% fetal bovine serum (FBS) in petri dishes in an incubator at 37°C. Using trypsin, the cells were detached from the petri dishes to incubate them in the fibers.

These cells are now ready to be transferred to the six well dish. Fibers were cut in $1cm^2$ squares and placed under UV light for 5 minutes.

Experiment setting preparation:

A six well dish was prepared for experimentation by placing coverslips in the wells and placing the previously 1cm fibers on the coverslips in the wells. The fibers were wetted using PBS buffer, the cells were added to each fiber in each well and left in the incubator for 1, 3, and 5 days.

Once the required amount of incubation time for the experiment has passed the cells were fixed and dyed using MTR and DAPI. The cells are first dyed with MTR for 20 minutes and washed with media two times for 7 minutes each. Then the cells are washed two times for two minutes with 1X PBS and fixed using a 4% formaldehyde solution for at least 30 minutes in the freezer (check temperature 4°C) The plate is washed two times for two minutes with PBS then DAPI is added for 5 minutes and a coverslip on top to assure equal dispersion, the coverslips are removed then the fibers with the cells are washed two times with PBS for two minutes. Finally, the coverslips with the cells and the fibers are mounted in a slide for later microscope analysis.

Antimicrobial Activity

The different samples were cut in a circle with a 1cm diameter. The gram-negative bacteria *Escherichia Coli (E. coli)* ATCC 25922 was inoculated on the agar in all the petri dishes. The bacteria were let to grow for 2 days. One sample with a 1cm diameter was positioned in the center on each petri dish. The inhibition area was measured and data in the form of photo and distance from the fiber to the start of the bacteria growth was acquired.

CHAPTER V

RESULTS AND DISCUSSION

Photos of Fibers

This are photos of PVB, PVB/Polylysine, PVB/TA/Polylysine, PHB, PHB/Polylysine, PHB/TA/Polylysine, CH/PL/TA and CH/PL/TA/Polylysine fibers fabricated by Forcespinning®.

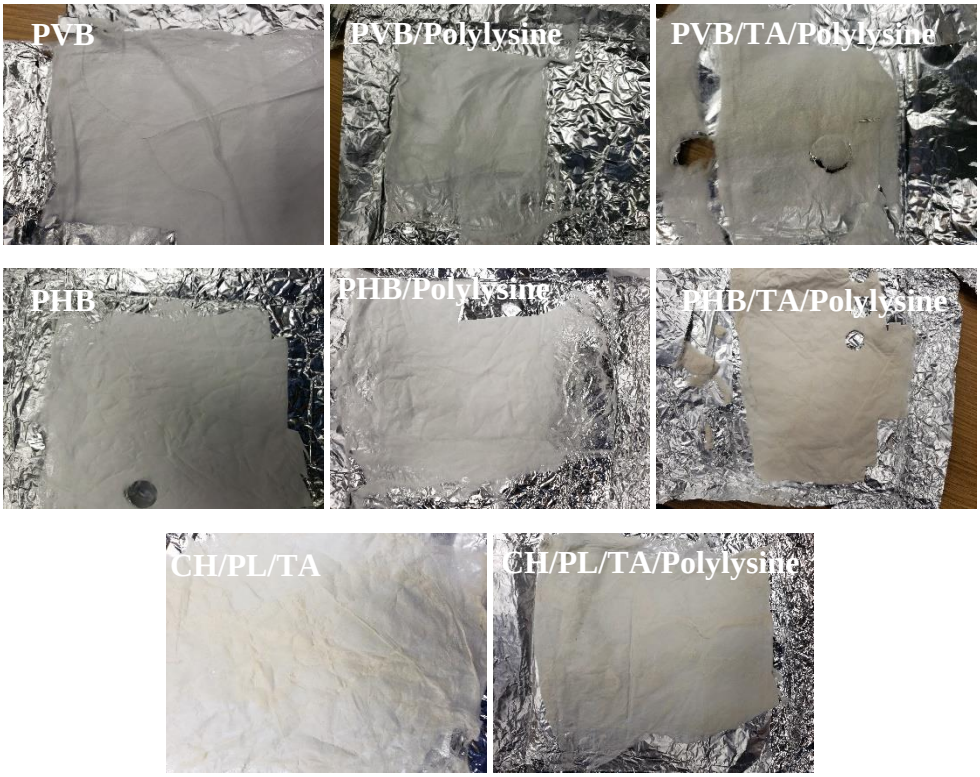

Figure 13. Photos of PVB, PVB/Polylysine, PVB/TA/Polylysine, PHB, PHB/Polylysine, PHB/TA/Polylysine, CH/PL/TA and CH/PL/TA/Polylysine fibers fabricated by Forcespinning®

SEM

The SEM images show the fiber morphology of the samples and help in the calculation of the average size diameter for each sample. Figure 14 shows the typical SEM images of the fibers made by using the Forcespinning® technology of the materials: PVB, PVB/Polylysine, PVB/TA/Polylysine, PHB, PHB/Polylysine, PHB/TA/Polylysine, CH/PL/TA and CH/PL/TA/Polylysine. The morphology is seeming to be one of a smooth, continuous and homogenous fibers for the fiber mats of PVB, PVB/Polylysine and PVB/TA/Polylysine fibers and CH/PL/TA and CH/PL/TA/Polylysine, however for PHB, PHB/Polylysine and PHB/TA/Polylysine fibers the SEM images show a rough surface with continuous and homogeneous fibers. (Refer to Appendix A for more images)

The distribution and average diameter of the different fibers samples are shown in Figure 15. PVB have an average diameter of 1.58 mm, PVB/Polylysine have an average diameter of 1.35 mm and PVB/TA/Polylysine have an average diameter of 1.50 mm, furthermore as shown in Figure 15 PVB the distribution of the fibers diameter average varies between the materials, being PVB the one with the widest range and PVB/TA/Polylysine with the smaller distribution. This suggest that the fiber diameter distribution is affected by the presence of polylysine and TA. Furthermore, PHB have an average diameter of 1.25mm, PHB/Polylysine of 2.32 mm, and PHB/TA/Polylysine have an average diameter of 2.24 mm. The distribution of the fiber diameter varies as well among the materials, we can observe that PHB have the smallest average diameter while PHB/Polylysine and PVB/TA/Polylysine have a wider distribution and a bigger average diameter suggesting that upon the addition of polylysine and TA the average diameter of the PHB fibers seems to increase. Finally, CH/PL/TA and CH/PL/TA/Polylysine had the smallest average diameter having

582 nm and 748 nm, respectively. The distribution for the CH/PL/TA fibers is narrower compared to the CH/PL/TA/Polylysine fibers. From the analysis it can be assumed that upon the addition of TA and polylysine to the CH/PL/TA composite the fibers diameter seems to increase as well as the distribution seems to get wider.

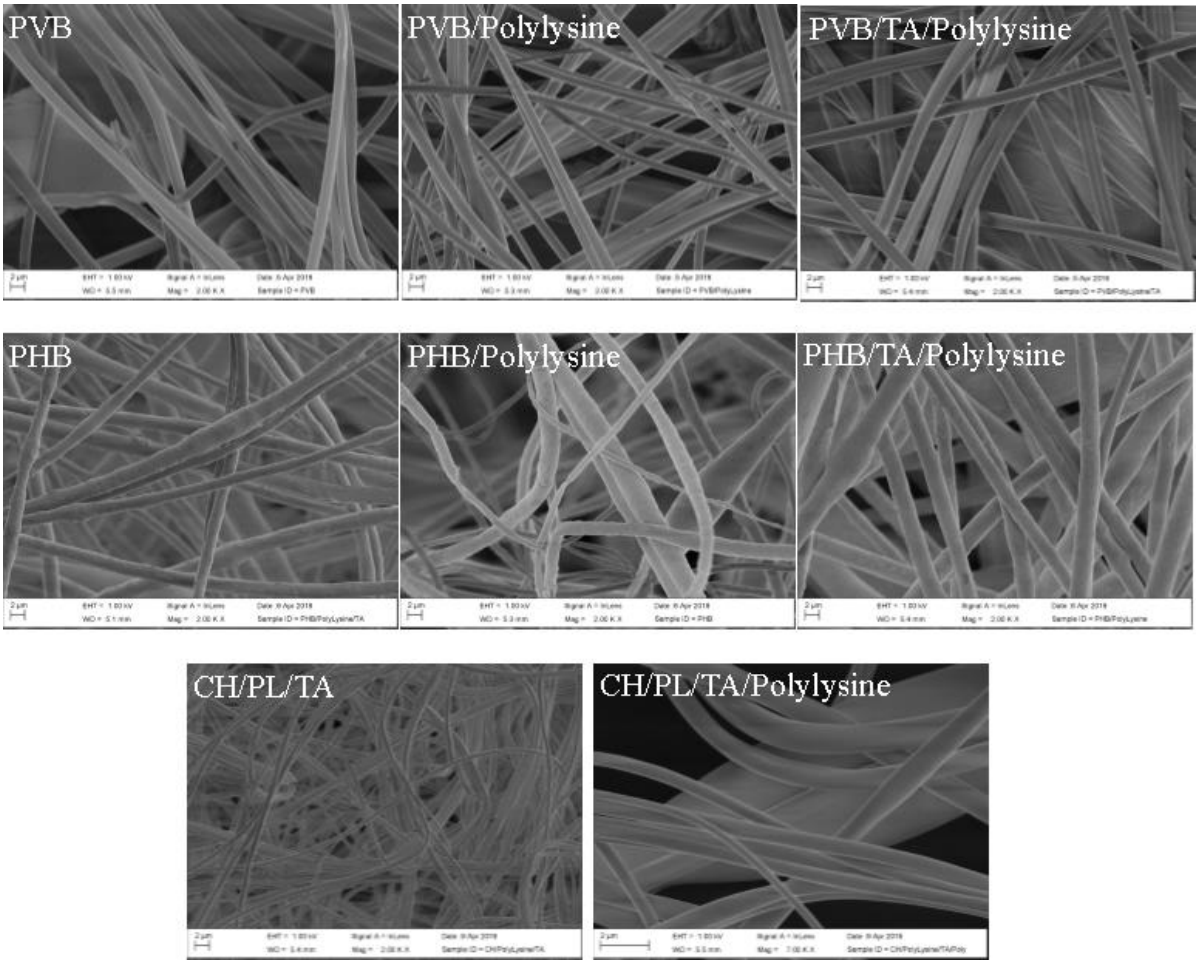

Figure 14. SEM images of PVB, PVB/Polylysine, PVB/TA/Polylysine, PHB, PHB/Polylysine, PHB/TA/Polylysine, CH/PL/TA and CH/PL/TA/Polylysine fibers fabricated by Forcespinning®

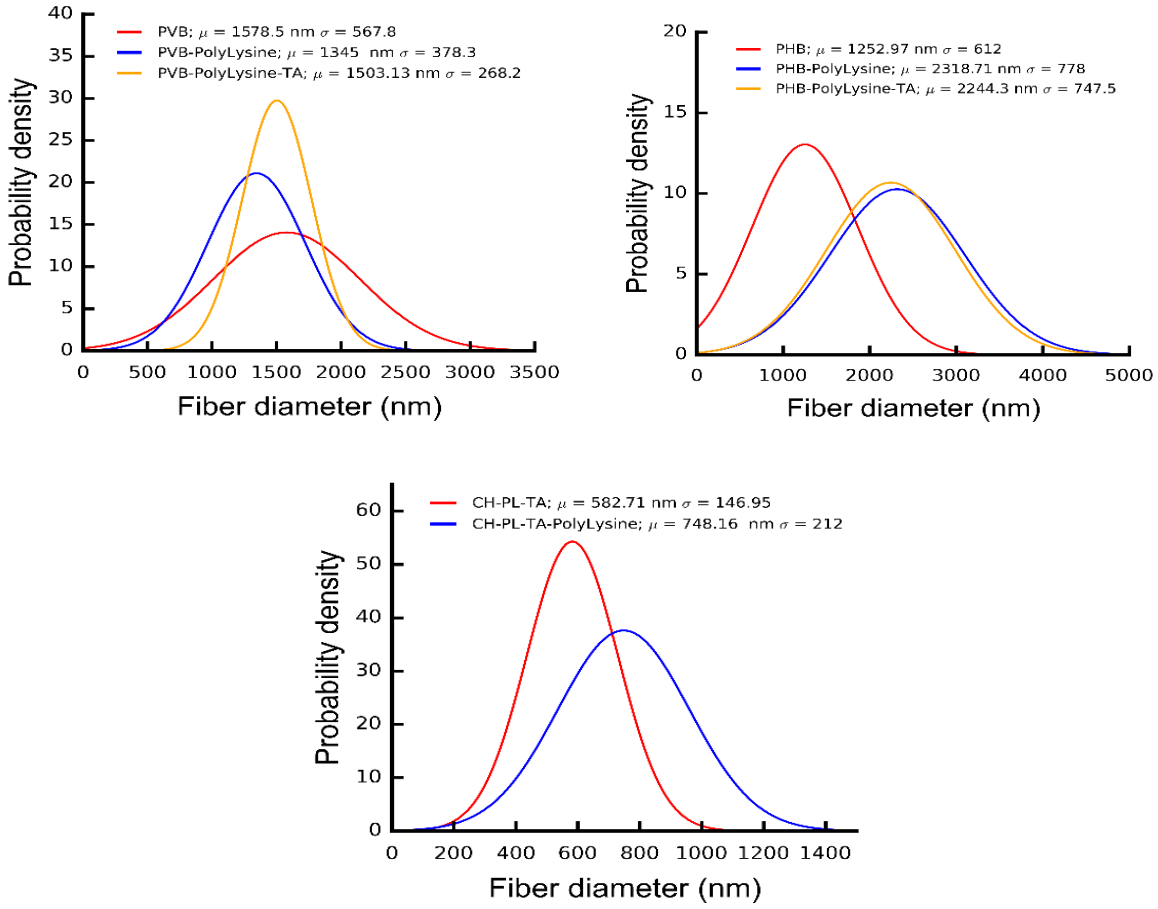

Figure 15. Average Diameter of PVB, PVB/Polylysine, PVB/TA/Polylysine, PHB, PHB/Polylysine, PHB/TA/Polylysine, CH/PL/TA and CH/PL/TA/Polylysine.

TGA

TGA was performed to understand the decomposition of the materials and to assure that no material is decomposing in an air environment at room temperature (RT).

TGA of PVB, PVB/Polylysine and PVB/TA/Polylysine

The TGA of PVB, PVB/Polylysine, and PVB/TA/Polylysine were performed in an air environment (Figure 16). Thermal stability can be observed from the TGA in air up to where the material starts to decompose with an onset point around 290°C. Similar onset points can be observed in through the different samples however some variations are obvious suggestion of a change in thermal stability and a shift of degradation to a higher temperature. The onset point for PVB are 290°C and 473°C, for PVB/Polylysine 311°C and 474 and for PVB/TA/Polylysine are 300°C and 472°C. The degradation of the butyral side groups is the larger mass loss shown between 290°C and 400°C where a second curve can be observed which can be attributed to the start of the loss of the acetate residues from of the polymer as found in the literature. [116]

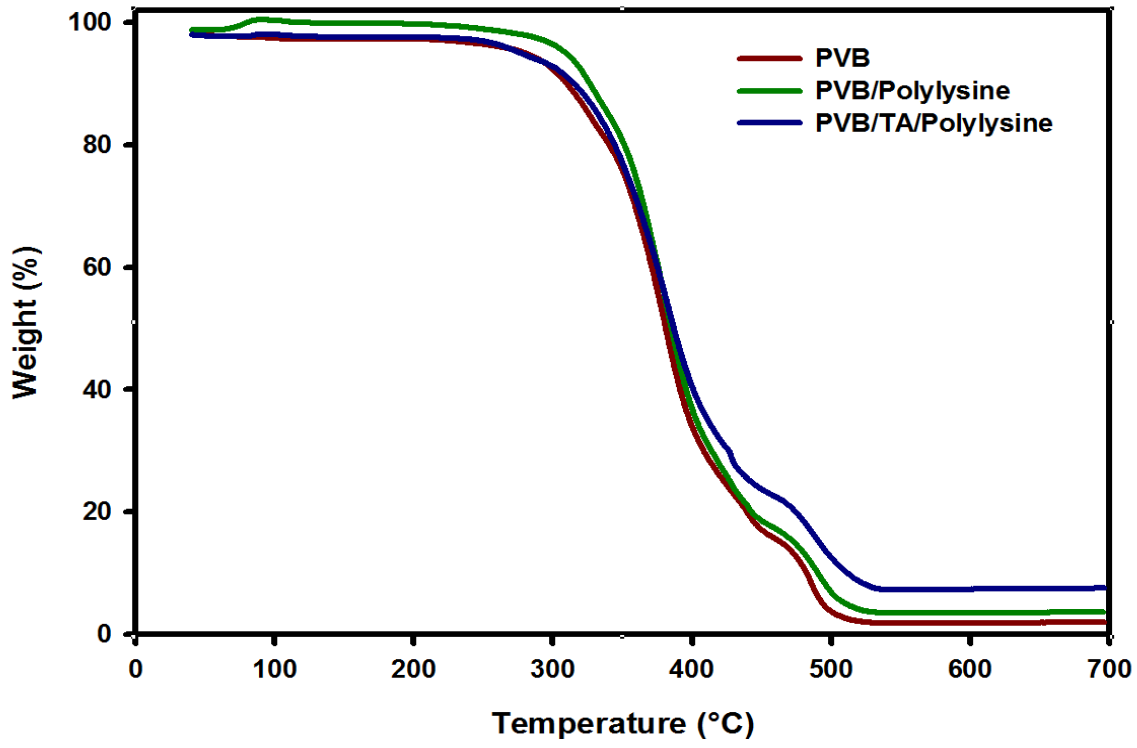

Figure 16. TGA of 1. PVB, PVB/Polylysine, PVB/TA/Polylysine

TGA of PHB, PHB/Polylysine and PHB/TA/Polylysine

TGA was run under air atmosphere (Figure17). The TGA shows how PHB starts degrading a lower temperature when compared to PVB however the material shows excellent thermal stability at RT. The onset point for pure PHB is 243°C while PHB/Polylysine have an onset point around 237°C and PHB/TA/Polylysine have an onset point around 257°C meaning that the PHB/TA/Polylysine have a better thermal stability than the pure PHB fibers while PHB/Polylysine starts degrading at lower temperature when compared to the PHB fibers. The material in the three samples are mostly degraded by 300°C, degradation attributed to random chain scission of the polymer [117], however they are not completely degraded until 450°C.

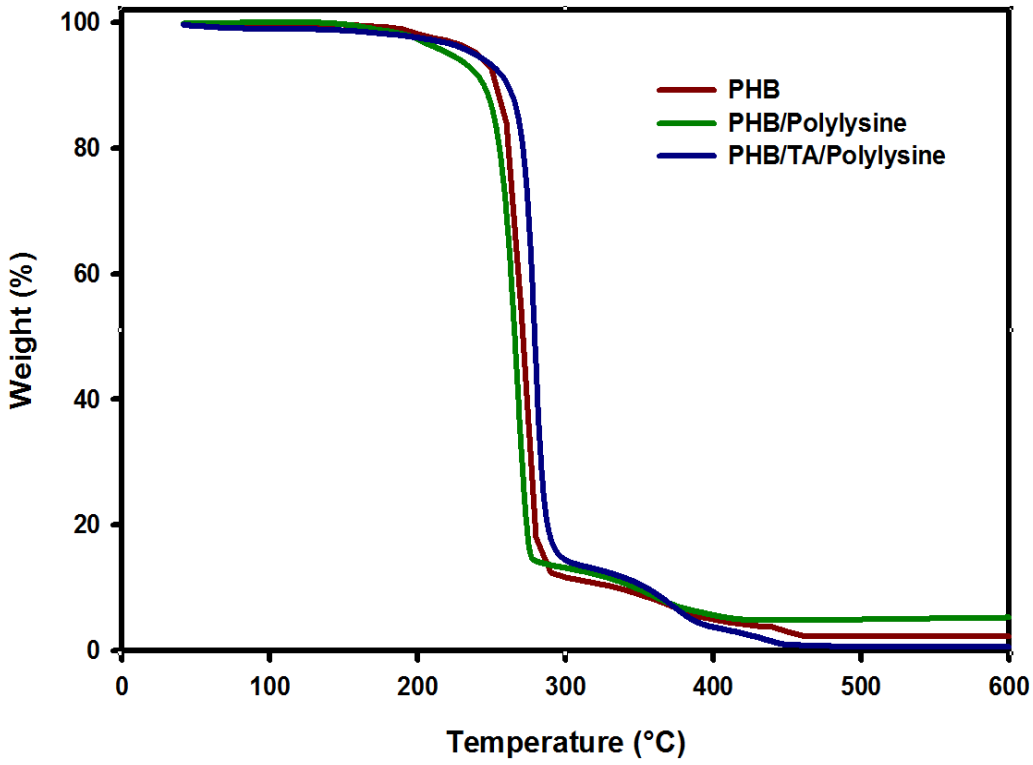

Figure 17. TGA of PHB, PHB/Polylysine and PHB/TA/Polylysine

TGA of CH/PL/TA and CH/PL/TA/Polylysine

The thermal stability of CH/PL/TA and CH/PL/TA/Polylysine is variable in the range of temperature studied (Figure 18). At 40°C, starting temperature of the TGA, a mass loss can be seem in the thermogram, though a higher loss of material is seem in the CH/PL/TA/Polylysine composite than the CH/PL/TA composite more studies will be needed to better understand the behavior. The onset point in the CH/PL/TA TGA graph is showed around 240°C and a second onset point is shown around 443°C while the onset points for CH/PL/TA/Polylysine are around 245°C and 430°C suggesting that upon the addition of Polylysine the thermal stability of the composite decreases by 5°C. Both materials are mostly degraded by 550°C, yet full degradation is seem in the CH/PL/TA/Polylysine.

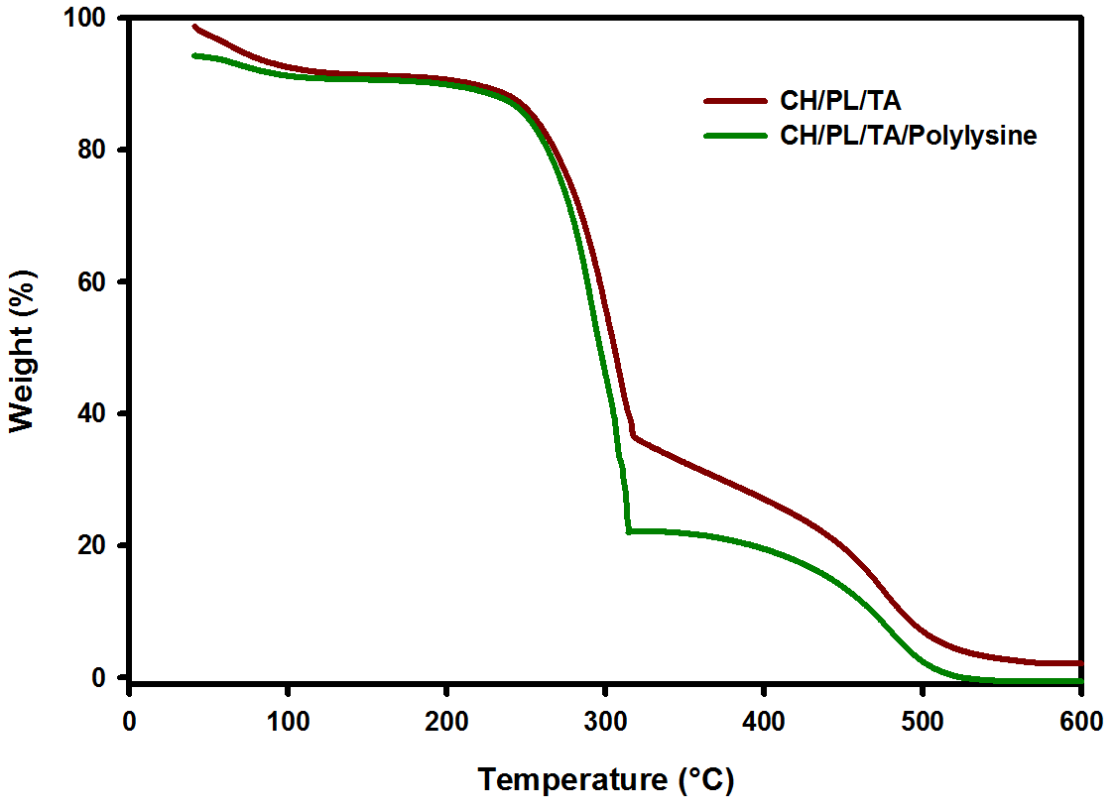

Figure 18. TGA of CH/PL/TA and CH/PL/TA/Polylysine

DSC

DSC of PVB, PVB/Polylysine and PVB/TA/Polylysine

DSC was performed to obtain a better understanding of the molecular elongation and movement of the polymer chains specifically its microstructure. PVB is an amorphous polymer, we can attribute the arrangement of the polymer (or meso-order) in the first cycle to the process that the polymer had to undergo during the rapid elongation from the spinneret due to the centrifugal forces exerted by the cyclone. The polymer PVB shows a natural glass transition temperature (Tg) around 69°C, which is decreased to 55°C which is expected due to the meso-order produces by the alignment of the polymer molecules into fibers. The same behavior is noted in the PVB/Polylysine and PVB/TA/Polylysine, where we can see that compared to PVB its natural Tg is higher being 71°C and 72°C respectively. The Tg of the materials decreases to 55°C for PVB, 57°C for PVB/Polylysine and 58°C for PVB/TA/Polylysine in the first cycle which could be attribute to the organization of the molecules into fibers. The Tg seems to be affected by the addition of polylysine and TA, being at a higher temperature when compared to PVB fibers, this can be due to this addition the polymer fibers need more energy (heat) to rearrange thus increasing the Tg. The first cycle and second cycle of the PVB, PVB/Polylysine and PVB/TA/Polylysine are shown in Figure 19.

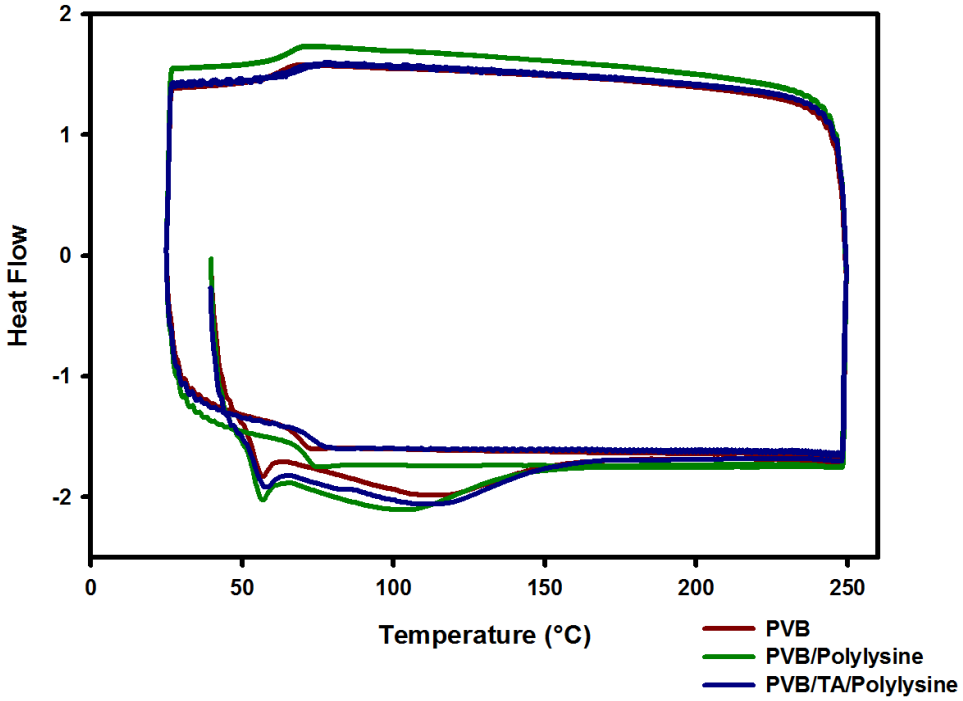

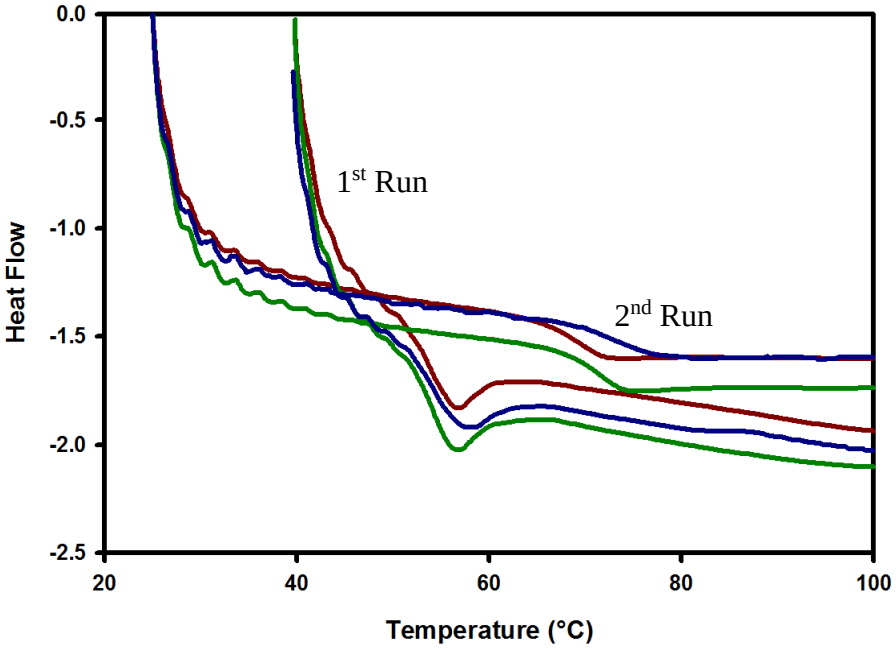

Figure 19. DSC of PVB, PVB/Polylysine, and PVB/TA/Polylysine

DSC of PHB, PHB/Polylysine and PHB/TA/Polylysine

PHB is a semi-crystalline material that have two different crystal structures, though more analysis is needed to know which crystal structures are present in the polymer. After the elongation of the molecules of the polymer chain into fibers, the crystals seem to arrange in a way that only one endothermic peak is present. By the shift of the exothermic peaks we can see that by the addition of polylysine it behaves as a nucleation agent shifting the peak to a higher crystallization temperature while by the addition of TA the peak seems to shift to the left, the same behavior as a plasticizer decreasing the crystallization temperature of the fibers as shown in Figure 20.

DSC of CH/PL/TA and CH/PL/TA/Polylysine

The DSC of CH/PL/TA and CH/PL/TA/Polylysine shows that the composite is amorphous and similar to the DSC of PVB, PVB/Polylysine and PVB/TA/Polylysine that due to the elongation after spinning the polymers into fibers the glass transition temperature is shifted to a lower temperature and a meso-order is obtained and is showed in the thermograph as an endothermic curve that can be appreciated in Figure 21.

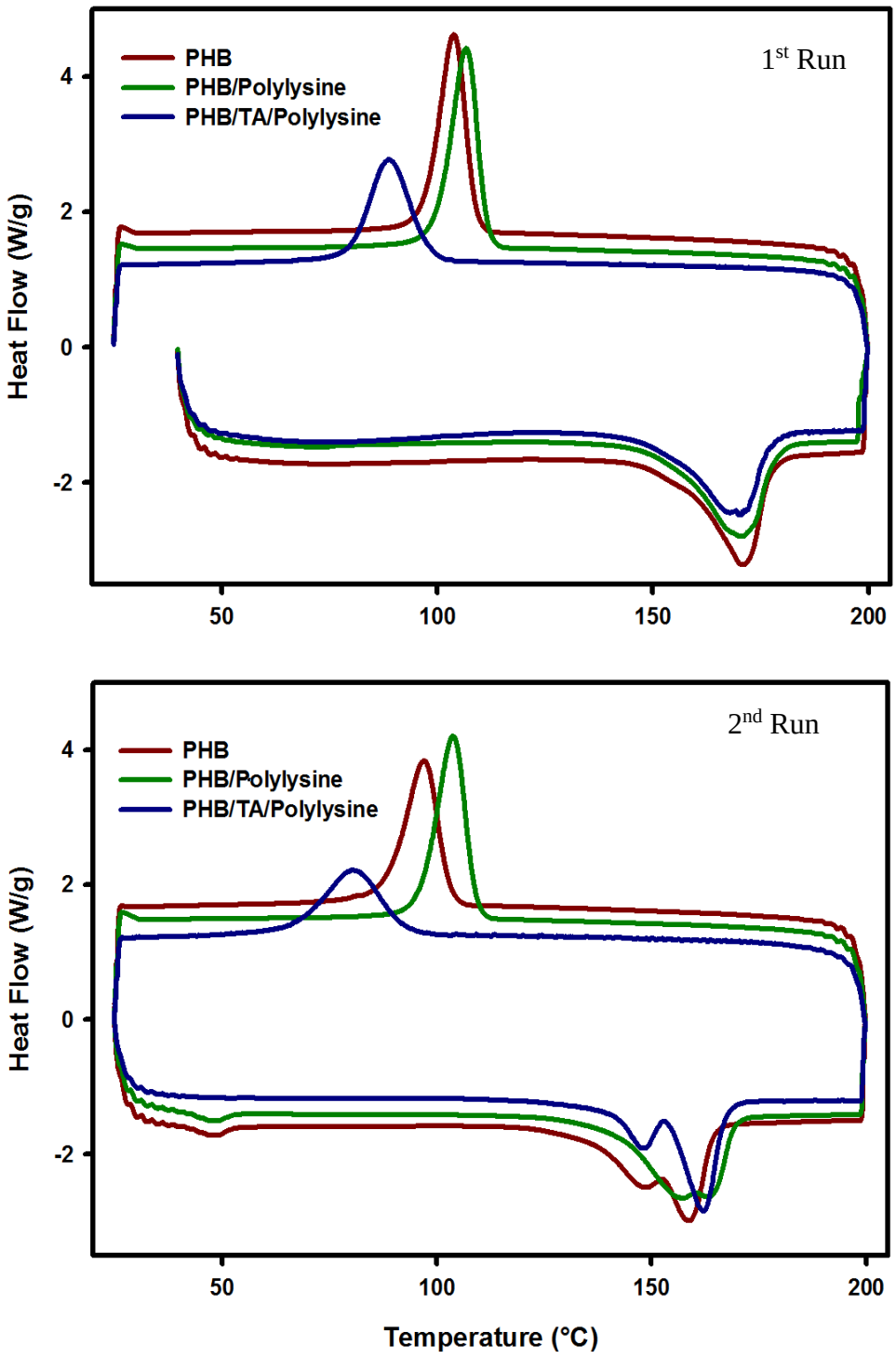

Figure 20. DSC of PHB, PHB/Polylysine, and PHB/TA/Polylysine

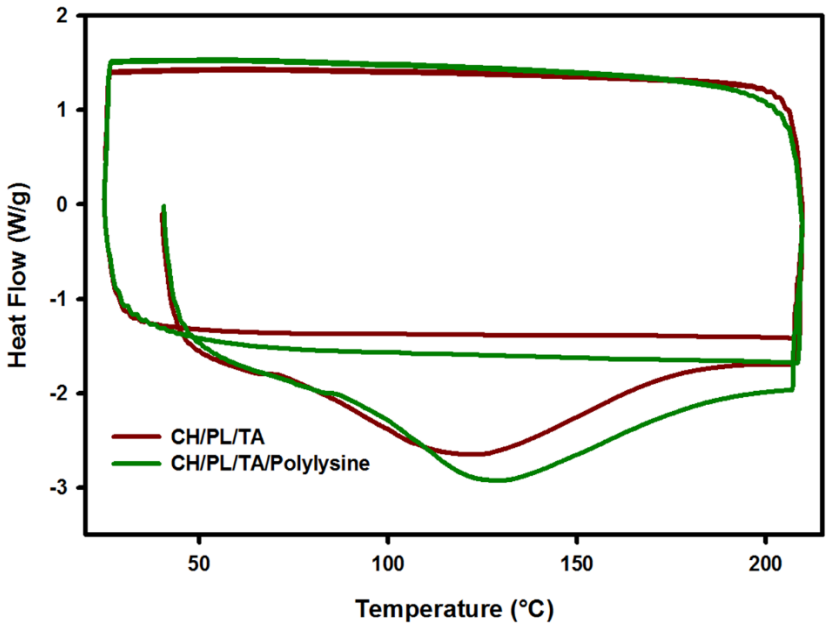

Figure 21. DSC of CH/PL/TA and CH/PL/TA/Polylysine

Contact Angle

Contact angle was performed to understand the relation between the hydrophobicity or hydrophilicity of the materials and its ability to function for cell growth in an in-vitro environment. Table 4 contains the results with the contact angle in degrees of the surfaces of PVB, PVB/Polylysine, PVB/TA/Polylysine PHB, PHB/Polylysine, PHB/TA/Polylysine, CH/PL/TA and CH/PL/TA/Polylysine with water.

PVB, PVB/Polylysine and PVB/TA/Polylysine fibers are hydrophobic with average of contact angle of 102°, 100° and 102°, respectively. PHB, PHB/Polylysine, PHB/TA/Polylysine fibers are hydrophobic as well with slightly lower average contact angles, 99° for PHB, 100° for PHB/Polylysine and 96° for PHB/TA/Polylysine. On the other hand, CH/PL/TA and CH/PL/TA/Polylysine fibers mat have a contact angle of 0°, making them super hydrophilic.

Table 4. Contact Angle of PVB, PVB/Polylysine, PVB/TA/Polylysine PHB, PHB/Polylysine, PHB/TA/Polylysine, CH/PL/TA and CH/PL/TA/Polylysine fibers with water.

Material/Polymer Mat	Average Contact Angle (degree)
PVB	102.59
PVB/Polylysine	100.7
PVB/TA/Polylysine	102.29
PHB	99.37
PHB/Polylysine	100.86
PHB/TA/Polylysine	96.82
CH/PL/TA	0
CH/PL/TA/Polylysine	0

Cell Growth

Cell growth experiments were performed using NIH 3T3 Mouse Embryonic Fibroblast cells. Cell adhesion was examined in a variety of fiber mats: of PVB, PVB/Polylysine, PVB/TA/Polylysine PHB, PHB/Polylysine, PHB/TA/Polylysine, CH/PL/TA and CH/PL/TA/Polylysine. The experiments show that upon the addition of polylysine and tannic acid cell growth and adhesion is not seeming to be inhibited. We found that in all cases the presence of polylysine does not significantly decrease the ability of 3T3 mouse embryonic fibroblasts to adhere to the fibers. P values were calculated using ANOVA biostatistical test.

Figure 22 shows the confocal visualization of the nucleus and mitochondrial morphology of embryonic fibroblast-3T3 cells on PVB, PVB/Polylysine, and PVB/TA/Polylysine using a FluoView FV10i-LIV Olympus® microscope. DAPI signaled blue for the nucleus, and Mito Tracker (MTR) signaled red for both the presence of mitochondria and fibers. Figure 23 shows the quantification of the 3T3 mouse embryonic fibroblast cells where there is no significant difference in cell adhesion among PVB fibers with or without polylysine and tannic acid which p value of 0.114 indicates no statistical difference between the samples.

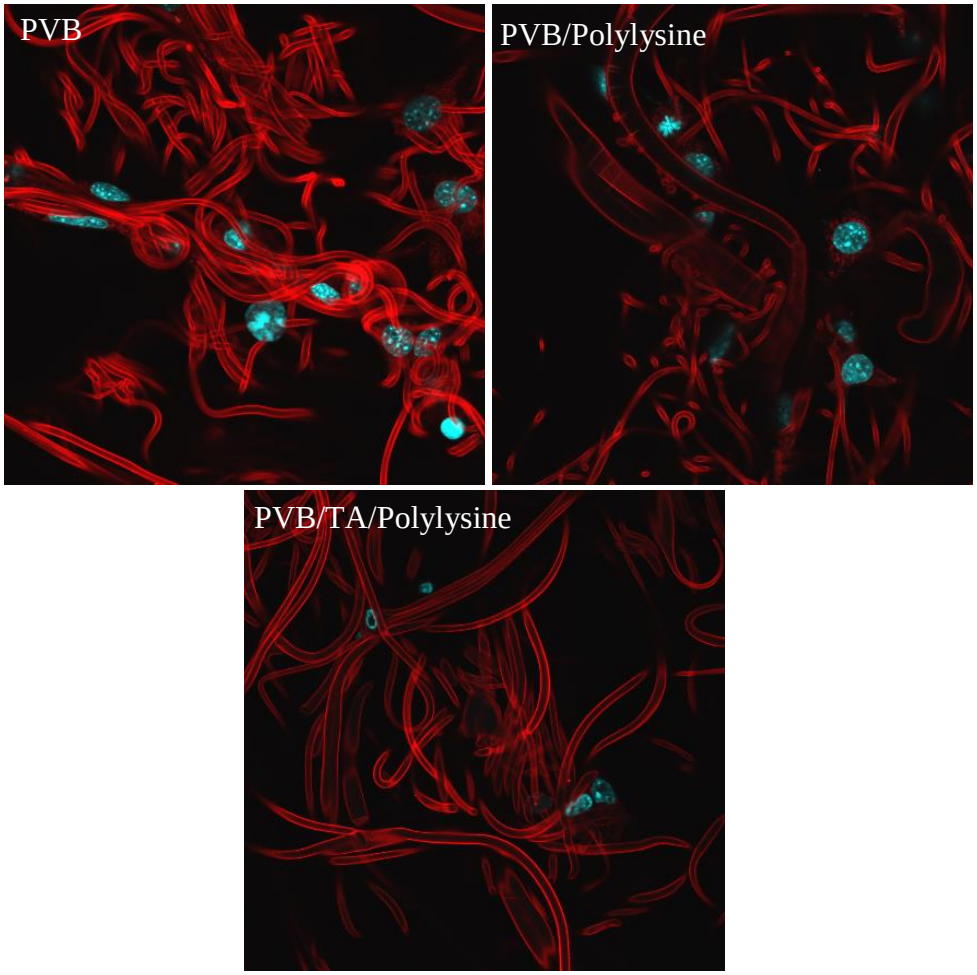

Figure 22. Confocal visualization of the nucleus and mitochondrial morphology of embryonic fibroblast-3T3 cells on PVB, PVB/Polylysine, and PVB/TA/Polylysine fibers. (n=3 experiments)

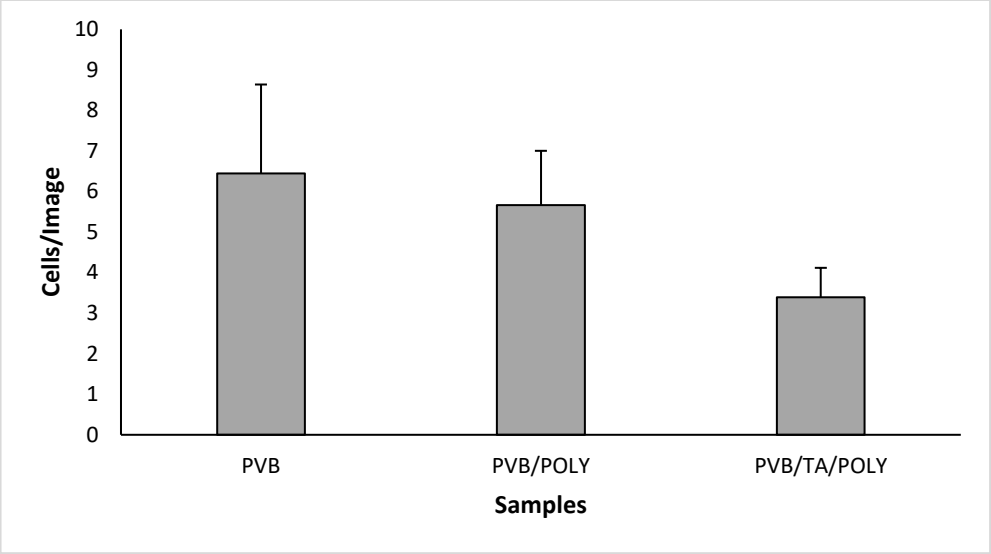

Figure 23. Quantitation of fibroblast-3T3 cells on PVB, PVB/Polylysine, and PVB/TA/Polylysine fibers

Polylysine does not seem to inhibit cell adhesion in the fibers of PHB, PHB/Polylysine and PHB/TA/Polylysine as showed in Figure 24; where a confocal visualization of the nucleus and mitochondrial morphology of embryonic fibroblast-3T3 cells on PHB, PHB/Polylysine, and PHB/TA/Polylysine using a FluoView FV10i-LIV Olympus® microscope. DAPI signaled blue for the nucleus, and Mito Tracker (MTR) signaled red for both the presence of mitochondria and the fibers. The p value is 0.081 which indicates that there is no significant difference in the cell count per image among these samples. This can be depicted in the graph in Figure 25, where an apparent increase in cell per image from PHB to PHB/Polylysine and a decrease by the addition of Tannic Acid, however the p value is 0.081 which $p>0.05$ which means that this values are statistically similar thus that the addition of polylysine and tannic acid are not inhibiting the ability of 3T3 fibroblast cells to adhere to the material.

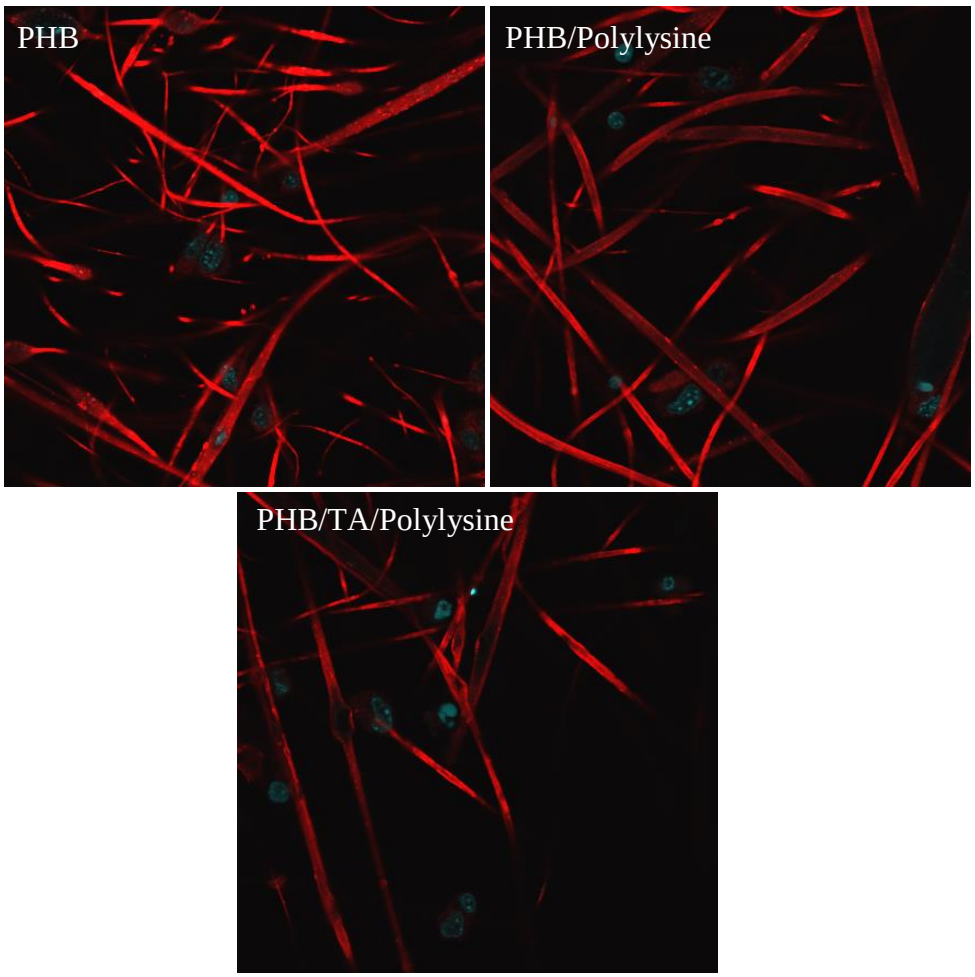

Figure 24. Confocal visualization of the nucleus and mitochondrial morphology of embryonic fibroblast-3T3 cells on PHB, PHB/Polylysine and PHB/TA/Polylysine fibers (n=3 experiments)

.

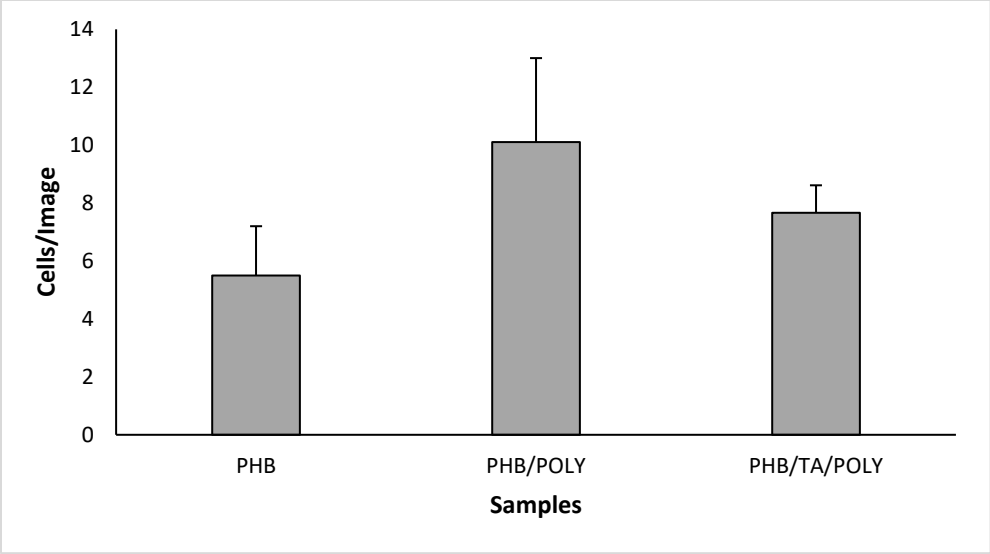

Figure 25. Quantitation of fibroblast-3T3 cells on PHB, PHB/Polylysine and PHB/TA/Polylysine fibers

A similar behavior can be observed in Figure 26 where 3T3 fibroblast cells in CH/PL/TA and CH/PL/TA/Polylysine fibers were a confocal visualization of the nucleus and mitochondrial morphology of embryonic fibroblast-3T3 cells on PHB, PHB/Polylysine, and PHB/TA/Polylysine using a FluoView FV10i-LIV Olympus® microscope. DAPI signaled blue for the nucleus, and Mito Tracker (MTR) signaled red for the presence of mitochondria. However, the nucleus in this samples did not get dyed properly by the DAPI which could be due to a human mistake factor. Figure 27 is a graphical representation of the quantitation of the cells per image in CH/PL/TA and CH/PL/TA fibers, where the p value is 0.374 which is greater than 0.05 showing that there is not significant difference between the samples in cell growth and adhesion, therefore indicating that the addition of polylysine to the CH/PL/TA composite does not inhibit the ability of 3T3 mouse embryonic fibroblast to adhere to the fiber mats.

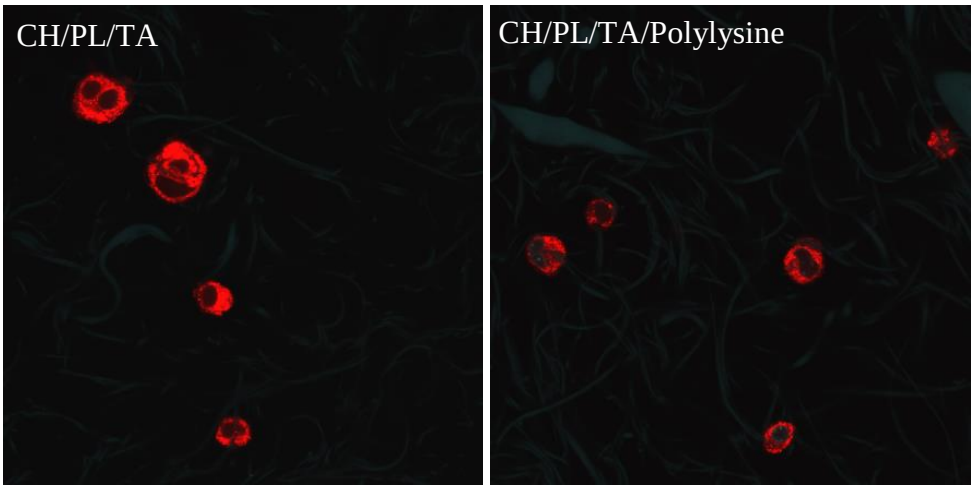

Figure 26. Confocal visualization of the nucleus and mitochondrial morphology of embryonic fibroblast-3T3 cells on CH/PL/TA and CH/PL/TA/Polylysine fibers. (n=3 experiments)

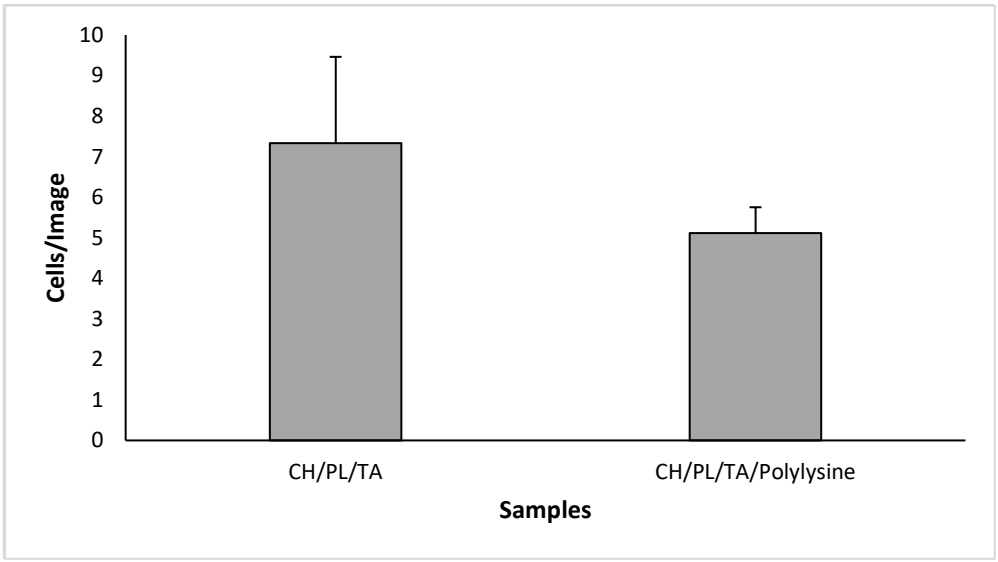

Figure 27. Quantitation of fibroblast-3T3 cells on CH/PL/TA and CH/PL/TA/Polylysine fibers.

Antimicrobial Activity

Figure 28 shows the antimicrobial experiment using *Escherichia coli* (*E. coli*) in the different fiber mats: PVB, PVB/Polylysine, PVB/TA/Polylysine, PHB, PHB/Polylysine, PHB/TA/Polylysine, CH/PL/TA and CH/PL/TA/Polylysine. The results show no inhibition of *E. coli* bacterial growth throughout the different samples.

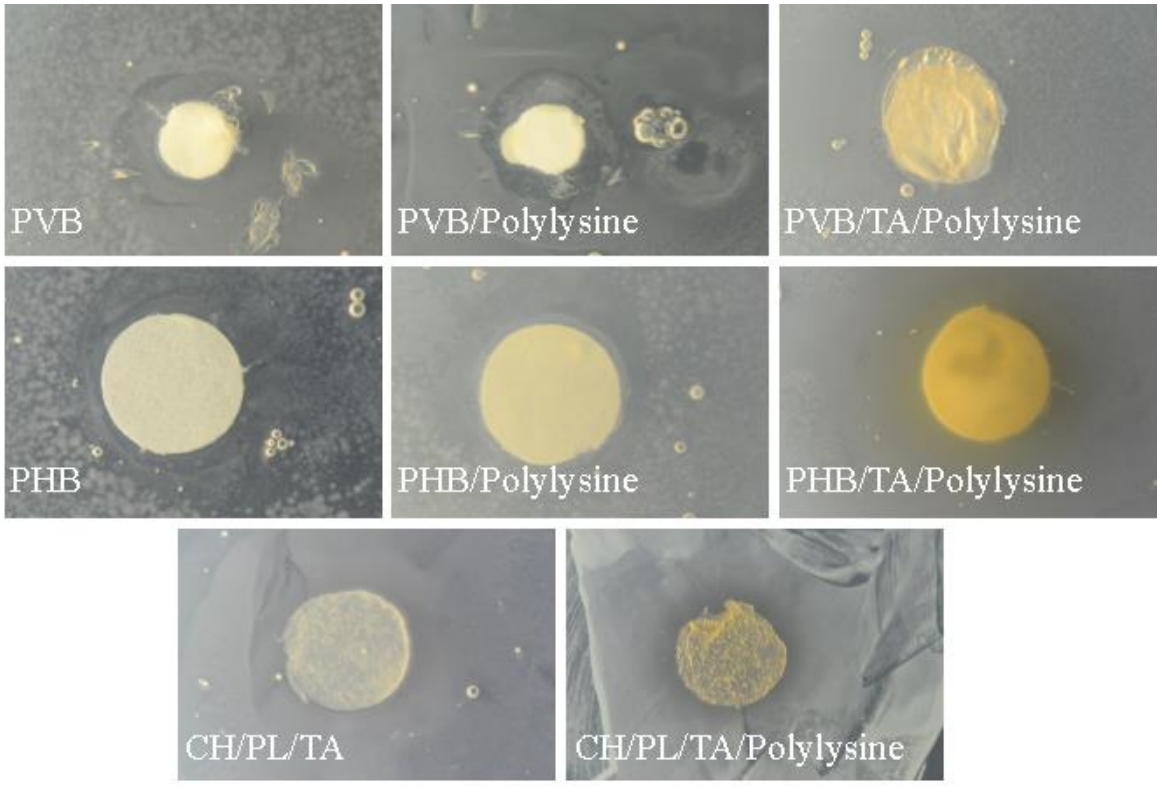

Figure 28. Antimicrobial activity of PVB, PVB/Polylysine, PVB/TA/Polylysine, PHB, PHB/Polylysine, PHB/TA/Polylysine, CH/PL/TA and CH/PL/TA/Polylysine fibers.

CHAPTER VI

CONCLUSION

Polymers spun using the Forcespinning® Technology could help increase cell growth. The polymers studied seems to mimic the extracellular matrix giving the cells a scaffold-like membrane to adhere and grow. These fibers show no antimicrobial activity against the gram-negative bacteria *Escherichia coli;* however, the addition of a better antimicrobial agent may help address this problem. PVB based fibers showed the possibility for this material to be used for bio-applications with ethanol as a solvent, giving the fiber the ability to withstand aqueous solutions and the presence of water without dissolving, as it would be in an open wound. PHB based fibers showed good cell adherence as well as CH/PL/TA based fibers. Studies show that the materials do not inhibit the ability of 3T3 mouse embryonic fibroblast cells to adhere to the fibers.

The studies showed great thermal stability with the lowest degradation on set point being 237 °C which shows that the materials are not decomposing at room temperature making them safe for the use of in-situ applications. DSC showed that upon the elongation produced by the Forscespinning® process the glass transition temperature seems to decrease giving the material the ability of flexibility which is desired for the application.

These studies indicate the use of fibers could enhance wound healing by giving the cells a 3D matrix to adhere and grow while having the plasticity needed to flex and fit into an acute

wound. However, more research is needed to understand the behavior of cell growth and to improve antibacterial activity, certainly TA should have had an effect, if the studies were properly conducted, then the concentration should have been increased or other additives could have been added.

REFERENCES

1. Martin, P. (1997). Wound Healing--Aiming for Perfect Skin Regeneration. Science, 276(5309), 75-81. doi:10.1126/science.276.5309.75

2. National Hospital Ambulatory Medical Care Survey: 2011 Emergency Department Summary Tables (accessed on January 30, 2016, at http://www.cdc.gov/nchs/ahcd/web_tables.htm#2011).

3. Data from the American Burn Association. Burn Incidence and Treatment in the United States: 2014 Fact Sheet; and American Burn Association. 2014 National Burn Repository Report of Data From 2004-2013. Chicago, The Association, 2014.

4. Gallico, G. G. (1985). Permanent coverage of large burn wounds with autologous cultured human epithelium. Plastic and Reconstructive Surgery, 76(5), 812. doi:10.1097/00006534-198511000-00093

5. Gopal, A., Kant, V., Gopalakrishnan, A., Tandan, S. K., & Kumar, D. (2014). Chitosan-based copper nanocomposite accelerates healing in excision wound model in rats. European Journal of Pharmacology, 731, 8-19. doi:10.1016/j.ejphar.2014.02.033

6. Ashfaq, M., Verma, N., & Khan, S. (2016). Copper/zinc bimetal nanoparticles-dispersed carbon nanofibers: A novel potential antibiotic material. Materials Science and Engineering: C, 59, 938-947. doi:10.1016/j.msec.2015.10.079

7. Kim, J. E., Lee, J. H., Kim, S. H., & Jung, Y. (2018). Skin Regeneration with Self-Assembled Peptide Hydrogels Conjugated with Substance P in a Diabetic Rat Model. Tissue Engineering Part A, 24(1-2), 21-33. doi:10.1089/ten.tea.2016.0517

8. Guo, S., & Dipietro, L. (2010). Factors Affecting Wound Healing. Journal of Dental Research, 89(3), 219-229. doi:10.1177/0022034509359125

9. Gurtner, G. C., Werner, S., Barrandon, Y., & Longaker, M. T. (2008). Wound repair and regeneration. Nature International Journal of Science, 453, 314-321.

10. Strbo, N., Yin, N., & Stojadinovic, O. (2014). Innate and Adaptive Immune Responses in Wound Epithelialization. Advances in Wound Care, 3(7), 492-501. doi:10.1089/wound.2012.043

11. Nosbaum, A., Prevel, N., Truong, H., Mehta, P., Ettinger, M., Scharschmidt, T. C., . . . Rosenblum, M. D. (2016). Cutting Edge: Regulatory T Cells Facilitate Cutaneous Wound Healing. The Journal of Immunology, 196(5), 2010-2014. doi:10.4049/jimmunol.1502139

12. Ramirez, H., Patel, S. B., & Pastar, I. (2014). The Role of TGFβ Signaling in Wound Epithelialization. Advances in Wound Care, 3(7), 482-491. doi:10.1089/wound.2013.0466

13. Turabelidze, A., & Dipietro, L. A. (2013). Inflammation and Wound Healing. Oral Wound Healing, 39-56. doi:10.1002/9781118704509.ch3

14. Amar, M. B., & Wu, M. (2014). Re-epithelialization: advancing epithelium frontier during wound healing. Journal of The Royal Society Interface, 11(93), 20131038-20131038. doi:10.1098/rsif.2013.1038

15. Tonnesen, M. G., Feng, X., & Clark, R. A. (2000). Angiogenesis in Wound Healing. Journal of Investigative Dermatology Symposium Proceedings, 5(1), 40-46.

16. Greaves, N. S., Ashcroft, K. J., Baguneid, M., & Bayat, A. (2013). Current understanding of molecular and cellular mechanisms in fibroplasia and angiogenesis during acute wound healing. Journal of Dermatological Science, 72(3), 206-217. doi:10.1016/j.jdermsci.2013.07.008

17. Darby, I. A., Laverdet, B., Bonté, F., & Desmouliere, A. (2014). Fibroblasts and myofibroblasts in wound healing. Clinical, Cosmetic and Investigational Dermatology, 7, 301-311. doi:10.2147/ccid.s50046

18. Hinz, B. (2007). Formation and Function of the Myofibroblast during Tissue Repair. Journal of Investigative Dermatology, 127(3), 526-537. doi:10.1038/sj.jid.5700613

19. Li, M., Zhao, Y., Hao, H., Han, W., & Fu, X. (2017). Theoretical and practical aspects of using fetal fibroblasts for skin regeneration. Ageing Research Reviews, 36, 32-41. doi:10.1016/j.arr.2017.02.005

20. Bahar, A. A., & Ren, D. (2013). Antimicrobial Peptides. Pharmaceuticals, 6(12), 1543-1575. doi:10.3390/ph6121543

21. Kang, H., Kim, C., Seo, C. H., & Park, Y. (2016). The therapeutic applications of antimicrobial peptides (AMPs): a patent review. Journal of Microbiology, 55(1), 1-12. doi:10.1007/s12275-017-6452-1

22. Agier, J., & Brzezińska-Błaszczyk, E. (2016). Cathelicidins and defensins regulate mast cell antimicrobial activity. Postępy Higieny i Medycyny Doświadczalnej, 70, 618-636. doi:10.5604/17322693.1205357

23. Fabisiak, A., Murawska, N., & Fichna, J. (2016). LL-37: Cathelicidin-related antimicrobial peptide with pleiotropic activity. Pharmacological Reports, 68(4), 802-808. doi:10.1016/j.pharep.2016.03.015

24. Xhindoli, D., Pacor, S., Benincasa, M., Scocchi, M., Gennaro, R., & Tossi, A. (2016). The human cathelicidin LL-37 — A pore-forming antibacterial peptide and host-cell modulator. Biochimica et Biophysica Acta (BBA) - Biomembranes, 1858(3), 546-566. doi:10.1016/j.bbamem.2015.11.003

25. Zhong, G., Cheng, J., Liang, Z. C., Xu, L., Lou, W., Bao, C., . . . Fan, W. (2017). Short Synthetic β-Sheet Antimicrobial Peptides for the Treatment of Multidrug-Resistant Pseudomonas aeruginosaBurn Wound Infections. Advanced Healthcare Materials, 6(7), 1601134. doi:10.1002/adhm.201601134

26. Mohamed, M. F., Abdelkhalek, A., & Seleem, M. N. (2016). Evaluation of short synthetic antimicrobial peptides for treatment of drug-resistant and intracellular Staphylococcus aureus. Scientific Reports, 6(1), 1-14. doi:10.1038/srep29707

27. Mahmoudi, M., Bonakdar, S., Shokrgozar, M. A., Aghaverdi, H., Hartmann, R., Pick, A., . . . Parak, W. J. (2014). Correction to Cell-Imprinted Substrates Direct the Fate of Stem Cells. ACS Nano, 8(10), 11023-11023. doi:10.1021/nn505574u

28. Murray, L. M., Nock, V., Evans, J. J., & Alkaisi, M. M. (2014). Bioimprinted polymer platforms for cell culture using soft lithography. *Journal of Nanobiotechnology, 12*(1). doi:10.1186/s12951-014-0060-6

29. Mashinchian, O., Bonakdar, S., Taghinejad, H., Satarifard, V., Heidari, M., Majidi, M., . . . Mahmoudi, M. (2014). Cell-Imprinted Substrates Act as an Artificial Niche for Skin Regeneration. *ACS Applied Materials & Interfaces, 6*(15), 13280-13292. doi:10.1021/am503045b

30. Kranz, I., Gonzalez, J. B., Dörfel, I., Gemeinert, M., Griepentrog, M., Klaffke, D., . . . Gross, U. (2009). Biological response to micron- and nanometer-sized particles known as potential wear products from artificial hip joints: Part II: Reaction of murine macrophages to corundum particles of different size distributions. Journal of Biomedical Materials Research Part A, 89A(2), 390-401. doi:10.1002/jbm.a.32121

31. Jia, F., Liu, X., Li, L., Mallapragada, S., Narasimhan, B., & Wang, Q. (2013). Multifunctional nanoparticles for targeted delivery of immune activating and cancer therapeutic agents. Journal of Controlled Release, 172(3), 1020-1034. doi:10.1016/j.jconrel.2013.10.012

32. Almeida, J. P., Figueroa, E. R., & Drezek, R. A. (2014). Gold nanoparticle mediated cancer immunotherapy. Nanomedicine: Nanotechnology, Biology and Medicine, 10(3), 503-514. doi:10.1016/j.nano.2013.09.011

33. Kalashnikova, I., Das, S., & Seal, S. (2015). Nanomaterials for wound healing: scope and advancement. Nanomedicine, 10(16), 2593-2612. doi:10.2217/nnm.15.82

34. Dai, T., Tanaka, M., Huang, Y., & Hamblin, M. R. (2011). Chitosan preparations for wounds and burns: antimicrobial and wound-healing effects. Expert Review of Anti-infective Therapy, 9(7), 857-879. doi:10.1586/eri.11.59

35. Azuma, K., Izumi, R., Osaki, T., Ifuku, S., Morimoto, M., Saimoto, H., . . . Okamoto, Y. (2015). Chitin, Chitosan, and Its Derivatives for Wound Healing: Old and New Materials. Journal of Functional Biomaterials, 6(1), 104-142. doi:10.3390/jfb6010104

36. Patrulea, V., Ostafe, V., Borchard, G., & Jordan, O. (2015). Chitosan as a starting material for wound healing applications. European Journal of Pharmaceutics and Biopharmaceutics, 97, 417-426. doi:10.1016/j.ejpb.2015.08.004

37. Caetano, G. F., Frade, M. A., Andrade, T. A., Leite, M. N., Bueno, C. Z., Moraes, Â M., & Ribeiro-Paes, J. T. (2014). Chitosan-alginate membranes accelerate wound healing. Journal of Biomedical Materials Research Part B: Applied Biomaterials, 103(5), 1013-1022. doi:10.1002/jbm.b.33277

38. Dai, T., Tegos, G. P., Burkatovskaya, M., Castano, A. P., & Hamblin, M. R. (2008). Chitosan Acetate Bandage as a Topical Antimicrobial Dressing for Infected Burns. Antimicrobial Agents and Chemotherapy, 53(2), 393-400. doi:10.1128/aac.00760-08

39. Zambito, Y. (2013). Nanoparticles Based on Chitosan Derivatives. Advances in Biomaterials Science and Biomedical Applications. doi:10.5772/54944

40. Makadia, H. K., & Siegel, S. J. (2011). Poly Lactic-co-Glycolic Acid (PLGA) as Biodegradable Controlled Drug Delivery Carrier. Polymers, 3(4), 1377-1397. doi:10.3390/polym3031377

41. Chereddy, Kiran Kumar, et al. “Combined effects of PLGA and vascular endothelial growth factor promote the healing of non-Diabetic and diabetic wounds.” Nanomedicine: Nanotechnology, Biology and Medicine, vol. 11, no. 8, 2015, pp. 1975–1984., doi:10.1016/j.nano.2015.07.006.

42. Chereddy, K. K., Her, C., Comune, M., Moia, C., Lopes, A., Porporato, P. E., . . . Préat, V. (2014). PLGA nanoparticles loaded with host defense peptide LL37 promote wound healing. Journal of Controlled Release, 194, 138-147. doi:10.1016/j.jconrel.2014.08.016

43. Bandurska, Katarzyna, et al. “Unique features of human cathelicidin LL-37.” BioFactors, vol. 41, no. 5, Oct. 2015, pp. 289–300., doi:10.1002/biof.1225.

44. Chaniotakis, Nikos, et al. “Dendrimers as tunable vectors of drug delivery systems and biomedical and ocular applications.” International Journal of Nanomedicine, 2015, p. 1., doi:10.2147/ijn.s93069.

45. Gajbhiye, Virendra, et al. “Dendrimers as therapeutic agents: a systematic review.” Journal of Pharmacy and Pharmacology, vol. 61, no. 8, Jan. 2009, pp. 989–1003., doi:10.1211/jpp/61.08.0002.

46. Kondiah, Pariksha, et al. “A Review of Injectable Polymeric Hydrogel Systems for Application in Bone Tissue Engineering.” Molecules, vol. 21, no. 12, 2016, p. 1580., doi:10.3390/molecules21111580.

47. Caló, E., & Khutoryanskiy, V. V. (2015). Biomedical applications of hydrogels: A review of patents and commercial products. European Polymer Journal, 65, 252-267. doi:10.1016/j.eurpolymj.2014.11.024

48. Rey-Rico, A., Madry, H., & Cucchiarini, M. (2016). Hydrogel-Based Controlled Delivery Systems for Articular Cartilage Repair. BioMed Research International, 2016, 1-12. doi:10.1155/2016/1215263

49. Bonferoni, M., Sandri, G., Dellera, E., Rossi, S., Ferrari, F., Mori, M., & Caramella, C. (2014). Ionic polymeric micelles based on chitosan and fatty acids and intended for wound healing. Comparison of linoleic and oleic acid. European Journal of Pharmaceutics and Biopharmaceutics, 87(1), 101-106. doi:10.1016/j.ejpb.2013.12.018

50. Eke, Gozde, et al. “Development of a UV crosslinked biodegradable hydrogel containing adipose derived stem cells to promote vascularization for skin wounds and tissue engineering.” Biomaterials, vol. 129, 2017, pp. 188–198., doi:10.1016/j.biomaterials.2017.03.021.

51. Volkova, N., Yukhta, M., Pavlovich, O., & Goltsev, A. (2016). Application of Cryopreserved Fibroblast Culture with Au Nanoparticles to Treat Burns. Nanoscale Research Letters, 11(1). doi:10.1186/s11671-016-1242-y

52. Akturk, O., Kismet, K., Yasti, A. C., Kuru, S., Duymus, M. E., Kaya, F., . . . Keskin, D. (2016). Collagen/gold nanoparticle nanocomposites: A potential skin wound healing biomaterial. Journal of Biomaterials Applications, 31(2), 283-301. doi:10.1177/0885328216644536

53. Mcveigh, H. (2011). Topical silver for preventing wound infection. International Journal of Evidence-Based Healthcare, 9(4), 454-455. doi:10.1111/j.1744-1609.2011.00245.x

54. Zhang, X., Shen, W., & Gurunathan, S. (2016). Silver Nanoparticle-Mediated Cellular Responses in Various Cell Lines: An in Vitro Model. International Journal of Molecular Sciences, 17(12), 1603. doi:10.3390/ijms17101603

55. Galandáková, A., Franková, J., Ambrožová, N., Habartová, K., Pivodová, V., Zálešák, B., . . . Ulrichová, J. (2016). Effects of silver nanoparticles on human dermal fibroblasts and epidermal keratinocytes. Human & Experimental Toxicology, 35(9), 946-957. doi:10.1177/0960327115611969

56. Sun, H., Gao, N., Dong, K., Ren, J., & Qu, X. (2014). Graphene Quantum Dots-Band-Aids Used for Wound Disinfection. ACS Nano, 8(6), 6202-6210. doi:10.1021/nn501640q

57. Capanni, C., Messori, L., Orioli, P., Chiti, F., Stefani, M., Ramponi, G., . . . Gabrielli, S. (2004). Investigation of the effects of copper ions on protein aggregation using a model system. Cellular and Molecular Life Sciences (CMLS), 61(7-8), 982-991. doi:10.1007/s00018-003-3447-3

58. Goodwin, D. G., Marsh, K. M., Sosa, I. B., Payne, J. B., Gorham, J. M., Bouwer, E. J., & Fairbrother, D. H. (2015). Interactions of Microorganisms with Polymer Nanocomposite Surfaces Containing Oxidized Carbon Nanotubes. Environmental Science & Technology, 49(9), 5484-5492. doi:10.1021/acs.est.5b00084

59. Forouhi, N. G., & Wareham, N. J. (n.d.). Epidemiology of diabetes. *Medicine (Abingdon), 42*(12), 698-702. doi:10.1016/j.mpmed.2014.09.007

60. Crews, R. T., Schneider, K. L., Yalla, S. V., Reeves, N. D., & Vileikyte, L. (2016). Physiological and psychological challenges of increasing physical activity and exercise in patients at risk of diabetic foot ulcers: A critical review. *Diabetes/Metabolism Research and Reviews, 32*(8), 791-804. doi:10.1002/dmrr.2817

61. Tavakol, S., Jalili-Firoozinezhad, S., Mashinchian, O., & Mahmoudi, M. (2016). Chapter 26 – Bioinspired Nanotechnologies for Skin Regeneration. In *Nanoscience in Dermatology* (pp. 337-352). Elsevier. doi:10.1016/B978-0-12-802926-8.00026-4

62. Lee, V., Singh, G., Trasatti, J. P., Bjornsson, C., Xu, X., Tran, T. N., . . . Karande, P. (2014). Design and Fabrication of Human Skin by Three-Dimensional Bioprinting. *Tissue Engineering Part C: Methods,20*(6), 473-484. doi:10.1089/ten.tec.2013.0335

63. Gao, B., Yang, Q., Zhao, X., Jin, G., Ma, Y., & Xu, F. (2016). 4D Bioprinting for Biomedical Applications. *Trends in Biotechnology, 34*(9), 746-756. doi:10.1016/j.tibtech.2016.03.004

64. Momeni, F., Hassani.n, S. M., Liu, X., & Ni, J. (2017). A review of 4D printing. Materials & Design, 122, 42-79. doi:10.1016/j.matdes.2017.02.068

65. Gao, B., Yang, Q., Zhao, X., Jin, G., Ma, Y., & Xu, F. (2016). 4D Bioprinting for Biomedical Applications. Trends in Biotechnology, 34(9), 746-756. doi:10.1016/j.tibtech.2016.03.004

66. You, J., Rafat, M., Almeda, D., Maldonado, N., Guo, P., Nabzdyk, C. S., . . . Auguste, D. T. (2015). PH-responsive scaffolds generate a pro-healing response. Biomaterials, 57, 22-32. doi:10.1016/j.biomaterials.2015.04.011

67. Ninan, N., Forget, A., Shastri, V. P., Voelcker, N. H., & Blencowe, A. (2016). Antibacterial and Anti-Inflammatory pH-Responsive Tannic Acid-Carboxylated Agarose Composite Hydrogels for Wound Healing. ACS Applied Materials & Interfaces, 8(42), 28511-28521. doi:10.1021/acsami.6b10491

68. Kim, T., Silva, J., & Jung, Y. (2011). Enhanced functional properties of tannic acid after thermal hydrolysis. *Food Chemistry, 126*(1), 116-120. doi:10.1016/j.foodchem.2010.10.086

69. Kim, T., Silva, J., Kim, M., & Jung, Y. (2010). Enhanced antioxidant capacity and antimicrobial activity of tannic acid by thermal processing. *Food Chemistry, 118*(3), 740-746. doi:10.1016/j.foodchem.2009.05.060

70. Xu, F., Weng, B., Materon, L. A., Gilkerson, R., & Lozano, K. (2014). Large-scale production of a ternary composite nanofiber membrane for wound dressing applications. *Journal of Bioactive and Compatible Polymers, 29*(6), 646-660. doi:10.1177/0883911514556959

71. Gao, W., Sun, L., Fu, X., Lin, Z., Xie, W., Zhang, W., . . . Chen, X. (2018). Enhanced diabetic wound healing by electrospun core–sheath fibers loaded with dimethyloxalylglycine. *Journal of Materials Chemistry B, 6*(2), 277-288. doi:10.1039/c7tb02342a

72. Katti, D. S., Robinson, K. W., Ko, F. K., & Laurencin, C. T. (2004). Bioresorbable nanofiber-based systems for wound healing and drug delivery: Optimization of fabrication parameters. *Journal of Biomedical Materials Research, 70B*(2), 286-296. doi:10.1002/jbm.b.30041

73. Kataria, K., Gupta, A., Rath, G., Mathur, R., & Dhakate, S. (2014). In vivo wound healing performance of drug loaded electrospun composite nanofibers transdermal patch. *International Journal of Pharmaceutics, 469*(1), 102-110. doi:10.1016/j.ijpharm.2014.04.047

74. Coşkun, G., Karaca, E., Ozyurtlu, M., Özbek, S., Yermezler, A., & Çavuşoğlu, I. (2014). Histological evaluation of wound healing performance of electrospun poly(vinyl alcohol)/sodium alginate as wound dressing in vivo. *Bio-Medical Materials and Engineering, 24*(2), 1527-1536. doi:0.3233/BME-130956

75. Patel, S., Kurpinski, K., Quigley, R., Gao, H., Hsiao, B. S., Poo, M., & Li, S. (2007). Bioactive Nanofibers: Synergistic Effects of Nanotopography and Chemical Signaling on Cell Guidance. *Nano Letters, 7*(7), 2122-2128. doi:10.1021/nl071182z

76. Kurpinski, K. T., Stephenson, J. T., Janairo, R. R., Lee, H., & Li, S. (2010). The effect of fiber alignment and heparin coating on cell infiltration into nanofibrous PLLA scaffolds. *Biomaterials,31*(13), 3536-3542. doi:10.1016/j.biomaterials.2010.01.062

77. Ahire, J. J., & Dicks, L. M. (2014). 2,3-Dihydroxybenzoic Acid-Containing Nanofiber Wound Dressings Inhibit Biofilm Formation by Pseudomonas aeruginosa. *Antimicrobial Agents and Chemotherapy, 58*(4), 2098-2104. doi:10.1128/aac.02397-13

78. Ahire, J. J., Hattingh, M., Neveling, D. P., & Dicks, L. M. (2016). Copper-Containing Anti-Biofilm Nanofiber Scaffolds as a Wound Dressing Material. *Plos One, 11*(3). doi:10.1371/journal.pone.0152755

79. Liu, Y., Sun, Q., Wang, S., Long, R., Fan, J., Chen, A., & Wu, W. (2016). Studies of Silk Fibroin/Poly(Lactic-Co-Glycolic Acid) Scaffold, Prepared by Thermally Induced Phase Separation, as a Possible Wound Dressing. *Science of Advanced Materials, 8*(5), 1045-1052. doi:10.1166/sam.2016.2693

80. Xu, F., Weng, B., Materon, L. A., Gilkerson, R., & Lozano, K. (2014). Large-scale production of a ternary composite nanofiber membrane for wound dressing applications. *Journal of Bioactive and Compatible Polymers, 29*(6), 646-660. doi:10.1177/0883911514556959

81. Xu, F., Weng, B., Gilkerson, R., Materon, L. A., & Lozano, K. (2015). Development of tannic acid/chitosan/pullulan composite nanofibers from aqueous solution for potential applications as wound dressing. *Carbohydrate Polymers, 115*, 16-24. doi:10.1016/j.carbpol.2014.08.08

82. Xu, F., Weng, B., Materon, L. A., Kuang, A., Trujillo, J. A., & Lozano, K. (2016). Fabrication of cellulose fine fiber based membranes embedded with silver nanoparticles via Forcespinning. *Journal of Polymer Engineering, 36*(3). doi:10.1515/polyeng-2015-0092

83. Mamidi, N., Gutiérrez, H. M., Villela-Castrejón, J., Isenhart, L., Barrera, E. V., & Elías-Zúñiga, A. (2017). Fabrication of gelatin-poly(epichlorohydrin-co-ethylene oxide) fiber scaffolds by Forcespinning® for tissue engineering and drug release. *MRS Communications, 7*(04), 913-921. doi:10.1557/mrc.2017.117

84. Tal, H., Moses, O., Kozlovsky, A., & Nemcovsky, C. (2012). Bioresorbable Collagen Membranes for Guided Bone Regeneration. *Bone Regeneration*. doi:10.5772/34667

85. Ma, G., Yang, D., Wang, K., Han, J., Ding, S., Song, G., & Nie, J. (2010). Organic-soluble chitosan/polyhydroxybutyrate ultrafine fibers as skin regeneration prepared by electrospinning. *Journal of Applied Polymer Science, 118*(6), 3619-3624. doi:10.1002/app.32671

86. Yalcinkaya, F., Yalcinkaya, B., & Maryska, J. (2016). Preparation and Characterization of Polyvinyl Butyral Nanofibers Containing Silver Nanoparticles. *Journal of Materials Science and Chemical Engineering, 04*(01), 8-12. doi:10.4236/msce.2016.41002

87. Cinatl, J., & Cinatl, J. (1995). U.S. Patent No. 5,393,668. Washington, DC: U.S. Patent and Trademark Office. "Cultivation of mammalian cells in a protein-free medium on a polyvinylformal and/or polyvinyl butyral surface." Grant-US005393668A

88. Taylor, A. C. (1970). Adhesion Of Cells To Surfaces. *Adhesion in Biological Systems,* 51-71. doi:10.1016/b978-0-12-469050-9.50008-9

89. Mazia, D. (1975). Adhesion of cells to surfaces coated with polylysine. Applications to electron microscopy. *The Journal of Cell Biology, 66*(1), 198-200. doi:10.1083/jcb.66.1.198

90. Wittke, J. H. (2012, February 08). Introduction. Retrieved January 15, 2018, from http://saturno.fmc.uam.es/web/superficies/instrumentacion/Instrumentation.htm

91. University of Nebraska-Lincoln | Web Developer Network. (n.d.). SEM. Retrieved January 15, 2018, from https://ncmn.unl.edu/enif/microscopy/SEM.shtml

92. Carl Zeiss NTS Limited, "Operator's User Guide", en01, May 2011. 33

93. Joy, D. C., Lyman, C. E., Echlin, P., Lifshin, E., Sawyer, L., & Michael, J. (2003). The SEM and Its Modes of Operation. In J. Goldstein & D. E. Newbury (Authors), Scanning electron microscopy and x-ray microanalysis (3rd ed., pp. 61-98). NY, NY: Springer. doi:10.1007/978-1-4615-0215-9

94. Joy, D. C., Lyman, C. E., Echlin, P., Lifshin, E., Sawyer, L., & Michael, J. (2003). Electron Beam–Specimen Interactions. In J. Goldstein & D. E. Newbury (Authors), Scanning electron microscopy and x-ray microanalysis (3rd ed., pp. 61-98). NY, NY: Springer. doi:10.1007/978-1-4615-0215-9

95. Adams, B. L., & Field, D. P. (2009). Present State of Electron Backscatter Diffraction and Prospective Developments. In A. J. Schwartz & M. Kumar (Authors), Electron backscatter diffraction in materials science (2nd ed., pp. 1-20). New York: Springer. doi:10.1007/978-0-387-88136-2

96. Joy, D. C., Lyman, C. E., Echlin, P., Lifshin, E., Sawyer, L., & Michael, J. (2003). Image Formation and Interpretation. In J. Goldstein & D. E. Newbury (Authors), Scanning electron microscopy and x-ray microanalysis (3rd ed., pp. 99-193). NY, NY: Springer. doi:10.1007/978-1-4615-0215-9

97. McSwiggen, P. (2005). Tech Notes/WDS vs EDS. Retrieved January 23, 2018, from http://www.mcswiggen.com/TechNotes/WDSvsEDS.htm

98. Swapp, S. (2017, May 26). Scanning Electron Microscopy (SEM). Retrieved February 02, 2018, from https://serc.carleton.edu/research_education/geochemsheets/techniques/SEM.html

99. Doyle, H. (n.d.). Experimental Method and Testing Procedures - Laboratory 10: Thermogravimetric Analysis. Retrieved January 23, 2018, from https://sites.google.com/a/iastate.edu/laboratory-10-thermogravimetric analysis/experimental-methods

100. Hatakeyama, T., & Quinn, F. X. (1999). Thermogravimetry. In Thermal analysis: fundamentals and applications to polymer science (2nd ed., pp. 45-71). Chichester: John Wiley & Sons.

101. Mohomed, (n.d.). Thermogravimetric Analysis (TGA) Theory and Applications. Lecture presented at TA Instruments –Waters LLC. Retrieved from file:///C:/Users/User/Downloads/CA-2016-TGA%20(1).pdf

102. PerkinElmer, Inc. (n.d.). Differential Scanning Calorimetry (DSC) A Beginner's Guide. Retrieved from https://www.perkinelmer.com/CMSResources/Images/44-74542GDE_DSCBeginnersGuide.pdf

103. Steinmann, W., Walter, S., Beckers, M., Seide, G., & Gries, T. (2013). Thermal Analysis of Phase Transitions and Crystallization in Polymeric Fibers. Applications of Calorimetry in a Wide Context - Differential Scanning Calorimetry, Isothermal Titration Calorimetry and Microcalorimetry. doi:10.5772/54063

104. Sarkar, K., Gomez, C., Zambrano, S., Ramirez, M., Hoyos, E. D., Vasquez, H., & Lozano, K. (2010). Electrospinning to Forcespinning™. Materials Today, 13(11), 12-14. doi:10.1016/s1369-7021(10)70199-1

105. Padron, S., Fuentes, A., Caruntu, D., & Lozano, K. (2013). Experimental study of nanofiber production through forcespinning. Journal of Applied Physics, 113(2), 024318. doi:10.1063/1.4769886

106. Doan, H. N., Tsuchida, H., Iwata, T., Kinashi, K., Sakai, W., Tsutsumi, N., & Huynh, D. P. (2017). Fabrication and photochromic properties of Forcespinning® fibers based on spiropyran-doped poly(methyl methacrylate). RSC Advances, 7(53), 33061-33067. doi:10.1039/c7ra03794e

107. Doyle, H. (n.d.). Experimental Method and Testing Procedures - Laboratory 10: Thermogravimetric Analysis. Retrieved January 23, 2018, from https://sites.google.com/a/iastate.edu/laboratory-10-thermogravimetric analysis/experimental-methods

108. U.S. Department of Health and Human Services, Public Health Service, Centers for Disease Control and Prevention, & National Institutes of Health. (2000). Section III. In Primary Containment for Biohazards: Selection, Installation and Use of Biological Safety Cabinets (2nd ed., pp. 6-13). Washington: U.S. Government Printing Office.

109. U.S. Department of Health and Human Services, Public Health Service, Centers for Disease Control and Prevention, & National Institutes of Health. (2000). Section II. In Primary Containment for Biohazards: Selection, Installation and Use of Biological Safety Cabinets (2nd ed., pp. 3-4). Washington: U.S. Government Printing Office.

110. Fellers, T. J., & Davidson, M. W. (n.d.). Introduction to Confocal Microscopy. Retrieved from https://www.olympus-lifescience.com/en/microscope-resource/primer/techniques/confocal/confocalintro/

111. Paddock, S. W., Fellers, T. F., & Davidson, M. W. (n.d.). Introductory Confocal Concepts. Retrieved January 23, 2018, from https://www.microscopyu.com/techniques/confocal/introductory-confocal-concepts

112. Rosinger, A. (1944). U.S. Patent No. 2,350,534. Washington, DC: U.S. Patent and Trademark Office. "Magnetic Stirrer" Grant-US2350534A

113. Bates, M. K., D'Onofrio, J., Parrucci, M. L., & Wernerspach, D. (n.d.). Back to Basics: Proper Care and Maintenance for Your Cell Culture Incubator. *Technical Note: TNCO2CAREFEED 0514*. Incubators and Constant Temperature Thermo Fisher Scientific

114. Araújo, J. D., Menezes, J. D., Albuquerque, A. M., Almeida, O. D., & Araújo, F. U. (2013). Assessment and Certification of Neonatal Incubator Sensors through an Inferential Neural Network. *Sensors, 13*(11), 15613-15632. doi:10.3390/s131115613

115. Kwok, D., & Neumann, A. (1999). Contact angle measurement and contact angle interpretation. Advances in Colloid and Interface Science, 81(3), 167-249. doi:10.1016/s0001-8686(98)00087-6

116. Seo, J., Kuk, S., & Kim, K. (1997). Thermal decomposition of PVB (polyvinyl butyral) binder in the matrix and electrolyte of molten carbonate fuel cells. Journal of Power Sources, 69(1-2), 61-68. doi:10.1016/s0378-7753(97)02570-6

117. Aoyagi, Y., Yamashita, K., & Doi, Y. (2002). Thermal degradation of poly[(R)-3-hydroxybutyrate], poly[ε-caprolactone], and poly[(S)-lactide]. Polymer Degradation and Stability, 76(1), 53-59. doi:10.1016/s0141-3910(01)00265-8

APPENDIX A

APPENDIX A

BIOLOGICAL EXPERIMENTS

Other experiments were done to understand and draw a path for the experiments in this thesis. Experiments with 3T3 fibroblast cells in CH/PL/TA fibers, CH/PL/TA fibers dipped in Polylysine for 5 minutes, CH/PL/TA fibers dipped for 2 hours and CH/PL/TA/Polylysine fibers were performed and the images of the results are showed here (Figure 1). A quantitative analysis between CH/PL/TA labeled as "untreated" and CH/PL/TA dipped for two hours in polylysine is shown in Figure 2. Student T test was performed and a p value <0.05 was obtained suggesting that between the samples there is significant difference, thus there is a n increase in cell adhesion in the fibers dipped in polylysine for two hours compared to the CH/PL/TA untreated fibers.

Cell adherence of PVB fibers with different percentage of hydroxyl groups were exanimated PVB from Kuraray 60T had 5-6% more hydroxyl groups than PVB 60H. The resulting cell images are shown in Figure 3.

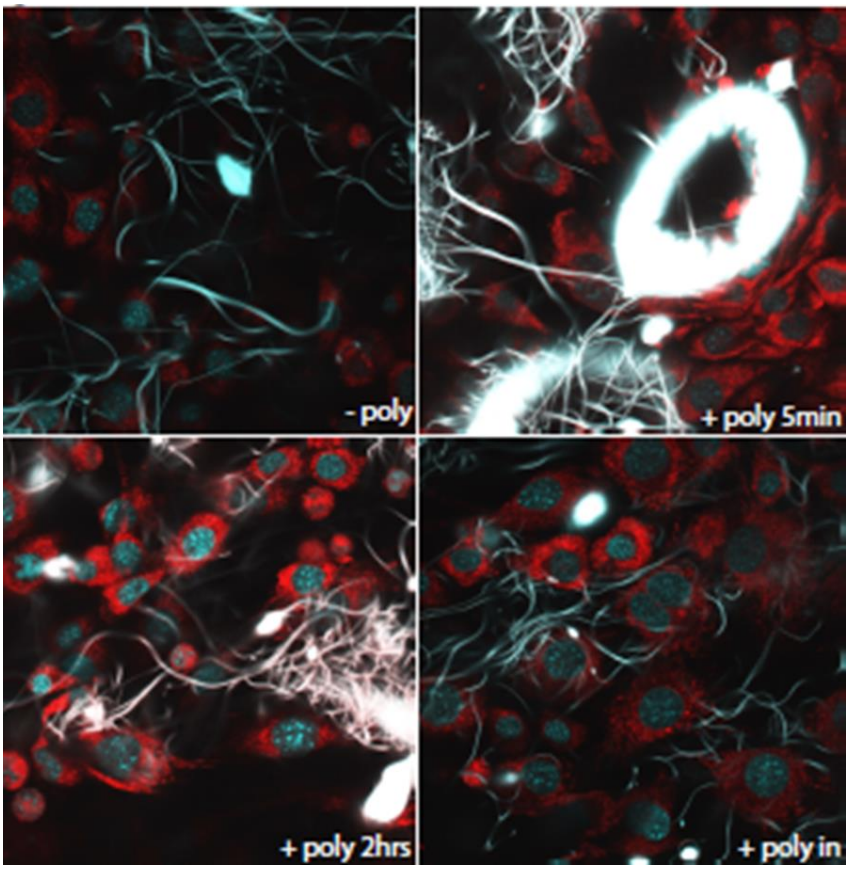

Figure 1. Confocal visualization of the nucleus and mitochondrial morphology of embryonic fibroblast-3T3 cells on CH/PL/TA fibers, CH/PL/TA fibers dipped in Polylysine for 5 minutes, CH/PL/TA fibers dipped for 2 hours and CH/PL/TA/Polylysine fibers.

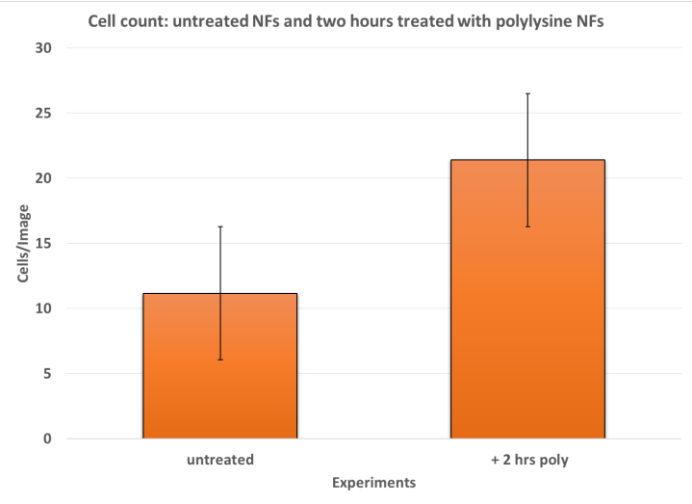

Figure 2. Quantitative analysis of cell growth of 3T3 fibroblast cells in untreated NFs and NFs treated with polylysine for two hours. Student's T-test: $p<0.05$ (n = 5 experiments).

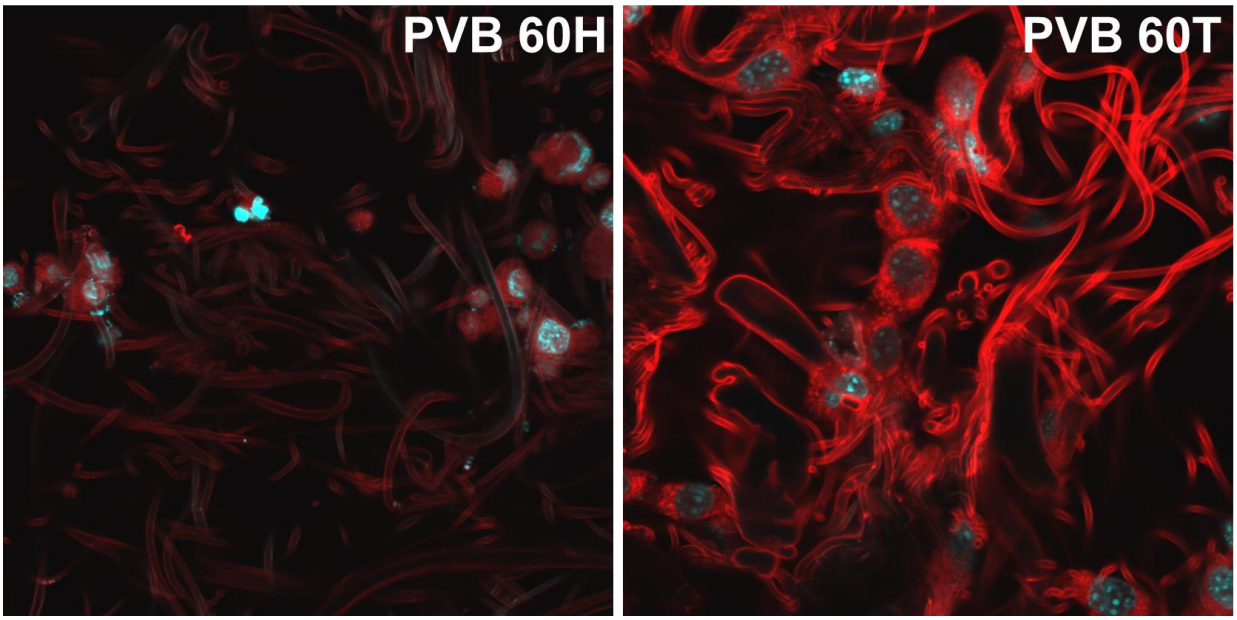

Figure 3. Confocal visualization of the nucleus and mitochondrial morphology of embryonic fibroblast-3T3 cells on PVB fibers.

APPENDIX B

APPENDIX B

STATE OF STATE-OF-THE-ART EQUIPMENT AND STATE-OF-THE-ART SOFTWARE

Table 1. State-of-the-Art Equipment.

Equipment	**Purpose**	**Results Obtained**
Forcespinning®	Development of PVB, PVB/Polylysine, PVB/TA/Polylysine, PHB, PHB/Polylysine, PHB/TA/Polylysine, CH/PL/TA and CH/PL/TA/Polylysine fibers.	PVB, PVB/Polylysine, PVB/TA/Polylysine, PHB, PHB/Polylysine, PHB/TA/Polylysine, CH/PL/TA and CH/PL/TA/Polylysine fibers were obtained.
Scanning Electron Microscope	Images of PVB, PVB/Polylysine, PVB/TA/Polylysine, PHB, PHB/Polylysine, PHB/TA/Polylysine, CH/PL/TA and CH/PL/TA/Polylysine fibers obtained through Forcespinning®.	PVB, PVB/Polylysine, PVB/TA/Polylysine, PHB, PHB/Polylysine, PHB/TA/Polylysine, CH/PL/TA and CH/PL/TA/Polylysine fibers images were obtained and analyzed and are included in Chapter 5 of the thesis.
Thermogravimetric Analyzer	Thermal degradation analysis of PVB, PVB/Polylysine, PVB/TA/Polylysine, PHB, PHB/Polylysine, PHB/TA/Polylysine, CH/PL/TA and CH/PL/TA/Polylysine fibers.	Temperatures of degradation of PVB, PVB/Polylysine, PVB/TA/Polylysine, PHB, PHB/Polylysine, PHB/TA/Polylysine, CH/PL/TA and CH/PL/TA/Polylysine fibers and are included in Chapter 5 of the thesis.

Differential Scanning Analyzer	Thermal analysis: measure glass transition temperature, melting and crystallization temperatures of PVB, PVB/Polylysine, PVB/TA/Polylysine, PHB, PHB/Polylysine, PHB/TA/Polylysine, CH/PL/TA and CH/PL/TA/Polylysine fibers.	Obtained the Glass Transition Temperature of PVB, PVB/Polylysine, PVB/TA/Polylysine, CH/PL/TA and CH/PL/TA/Polylysine fibers and melting and crystallization temperature of PHB, PHB/Polylysine and PHB/TA/Polylysine fibers and are included in Chapter 5 of the thesis.
Confocal Microscope	Visualization of Cells in PVB, PVB/Polylysine, PVB/TA/Polylysine, PHB, PHB/Polylysine, PHB/TA/Polylysine, CH/PL/TA and CH/PL/TA/Polylysine fibers.	Images of cells in PVB, PVB/Polylysine, PVB/TA/Polylysine, PHB, PHB/Polylysine, PHB/TA/Polylysine, CH/PL/TA and CH/PL/TA/Polylysine fibers and are included in Chapter 5 of the thesis.
Contact Angle	Measure the contact angle between PVB, PVB/Polylysine, PVB/TA/Polylysine, PHB, PHB/Polylysine, PHB/TA/Polylysine, CH/PL/TA and CH/PL/TA/Polylysine fibers and water.	Contact angles of PVB, PVB/Polylysine, PVB/TA/Polylysine, PHB, PHB/Polylysine, PHB/TA/Polylysine, CH/PL/TA and CH/PL/TA/Polylysine fibers a table with the results is included in Chapter 5 of the thesis.

Table 2. State-of-the-Art Software

Software	**Purpose**	**Results Obtained**
TA Analyzer Software	Analysis of TGA and DSC	TGA: onset point, temperature of degradation and residual percentage of material of PVB, PVB/Polylysine, PVB/TA/Polylysine, PHB, PHB/Polylysine, PHB/TA/Polylysine, CH/PL/TA and CH/PL/TA/Polylysine fibers included in Chapter 5 of the thesis. DSC: Glass transition temperature, melting and crystallization temperature of PVB, PVB/Polylysine, PVB/TA/Polylysine, PHB, PHB/Polylysine, PHB/TA/Polylysine, CH/PL/TA and CH/PL/TA/Polylysine fibers included in Chapter 5 of the thesis.
SigmaPlot	Analysis of experimental data	Graphing of Experimental Data presented in Chapter 5 of the thesis.
ImageJ	Analysis of SEM images	Average Diameter of PVB, PVB/Polylysine, PVB/TA/Polylysine, PHB, PHB/Polylysine, PHB/TA/Polylysine, CH/PL/TA and CH/PL/TA/Polylysine fibers included in Chapter 5 of the thesis.

BIOGRAPHICAL SKETCH

Astrid Michelle Rodriguez Negron was born in Caguas, Puerto Rico on May 18th, 1993. She went to a catholic elementary, middle and high school, Colegio San José Superior located in her hometown, Caguas, Puerto Rico from where she obtained her high school diploma in 2011. She then graduated with a Bachelor of Science in Cell and Molecular Biology in 2015 which she completed with a full institutional honor scholarship at Universidad Metropolitana in Cupey, San Juan, Puerto Rico. Astrid earned a Master of Science Engineering in Mechanical Engineering from the University of Texas Rio Grande Valley in May 2018.

An email for communication regarding the thesis is amrn230@gmail.com.